Available online at www.sciencedirect.com
SCIENCE DIRECT®
International Journal of Heat and Mass Transfer 48 (2005) 1608–1632
International Journal of HEAT and MASS TRANSFER
www.elsevier.com/locate/ijhmt

Modeling and effect of leakages on heat transfer performance of fixed matrix regenerators

Teodor Skiepko [a,*], Ramesh K. Shah [b]

[a] Bialystok Technical University, 15-351 Bialystok, Poland
[b] Rochester Institute of Technology, Rochester, NY 14623-5604, USA

Received 20 September 2003; received in revised form 21 July 2004

Abstract

The following undesired leakages are inherent in operation of fixed matrix regenerators: gas pressure leakages due to pressure difference such as leakages through the valves and through cracks in regenerator housing for very high temperature heat recovery, and carryover leakages from the hot gas to cold gas and vice versa. The objective of this paper is to present a methodology for evaluation of the leakages and to determine quantitatively the detrimental influence of pressure leakages on the regenerator heat transfer performance. In this respect, a drop (reduction) in actual regenerator heat transfer effectiveness due to various leakages is presented in the paper. The results clearly suggest that a drop in the effectiveness due to leakages can be significant and depends on the category of leakages. The flow leakages due to the cracks in the regenerator housing have the most impact on reducing the regenerator performance.

1. Introduction

The main advantage of the fixed-matrix regenerator is that it is probably the least expensive heat recovery installation to operate effectively in harsh operating conditions, such as withstanding extremely high or low temperatures, or corrosive and fouled gases as working fluids. One of the main drawbacks of the regenerators is the undesired leakages inherent in the operation. The pressure leakages occur due to the pressure difference between the hot and cold gases as well as between the hot and cold gases and the ambient. Also the gas trapped in the void volume of the matrix at the time of switching the valve/damper position is captured immediately from the matrix by the inflowing other gas stream. This leakage is referred to as *carryover leakage*. In a fixed-matrix regenerator, two or more matrices are used for continuous operation (Fig. 1). As shown in Fig. 1a, when the hot gas flows through matrix A, cold gas flows through matrix B, so that when matrix A is being heated, matrix B is being cooled and vice versa, as shown in Fig. 1b.

Referring to leakages marked in Fig. 1, valve pressure leakages and gas carryover for two neighbouring periods are the mirror images. However, the crack leakages are not the mirror images although they appear to be in Fig. 1. This is because usually, cracks in housing are at different places for either individual matrix and have different flow areas, and the leaking air and gas

* Corresponding author. Tel.: +48 85 746 92 71; fax: +48 85 742 92 10.
E-mail address: tskiepko@pb.bialystok.pl (T. Skiepko).

0017-9310/$ - see front matter © 2004 Elsevier Ltd. All rights reserved.
doi:10.1016/j.ijheatmasstransfer.2004.10.023

Nomenclature

A	leakage flow area, m^2
A_{fr}	frontal area of the regenerator, m^2
C_d	coefficient of discharge, dimensionless
C	fluid heat capacity rate, J/K
C_r	matrix heat capacity rate, J/K
C^*	heat capacity rate ratio, C_{min}/C_{max}, dimensionless
C_r^*	matrix heat capacity rate ratio, C_r/C_{min}, dimensionless
f	mass fraction, dimensionless
G	gas mass velocity based on minimum free-flow area, kg/m^2 K
G_{fr}	gas mass velocity based on frontal area, kg/m^2 K
h	heat transfer coefficient, W/m^2 K
H	enthalpy per unit mass, J/g
L	matrix height, m
$\dot{m}$	mass flow rate, g/s
$\dot{m}'$	gas mass flow rate in the matrix changed by the crack leakage, g/s
n	nth matrix layer number
N	total number of different matrix layers
NTU_o	modified overall number of transfer units, dimensionless
p	static pressure, Pa
Δp	pressure drop, Pa
P	duration of the period, s
P_{tot}	total period of operation, P_h+P_c, s
Q	amount of heat transferred per period, GJ/period
T	gas temperature, °C
T'	inlet/outlet or mixed gas temperatures for the internal regenerator, °C

Greek symbols

δ	semi-thickness of matrix elements, m
ε	regenerator heat transfer effectiveness, dimensionless
ε_b	effectiveness of the actual regenerator with leakages, dimensionless
λ	Darcy–Weisbach friction factor, dimensionless
ρ	mass density, kg/m^3
ρ'	inlet/outlet mass density for the internal regenerator, kg/m^3
σ	matrix porosity, dimensionless
ΔV	Volume in between the valve and matrix, m^3

Subscripts

a	ambient
a,cr	crack leakage of ambient air into the regenerator
c	cold gas or cold period
c,cr	crack leakage of the cold gas out of the regenerator
co	carryover
c,υ	cold end valve
C	convection mode
h	hot gas or hot period
h,υ	hot end valve
i	internal regenerator or inlet
jth	gas component
max	maximum value of (C_c,C_h)
min	minimum value of (C_c,C_h)
o	outlet
r	rotating matrix
R	thermal radiation mode
υ	valve
w	matrix material
CO_2	carbon dioxide
H_2O	water vapor
N_2	nitrogen
O_2	oxygen

Superscripts

(ℓ)	left regenerator
(r)	right regenerator
$\sim$	former period
(aυ)	averaged value
$'$	at inlet/outlet to/from internal regenerator
(1),...	parts (1) to (4) of the internal regenerator

are at different densities. As shown in Fig. 1a, ambient air leaks into the left matrix A and cold heated gas outflows from the right matrix B through the cracks in the housing during one period of operation. However, once the valves are switched, see Fig. 1b, the heated gas outflows from the left matrix A through the cracks and the ambient air flows into the matrix through the cracks in the right matrix B. Consequently, corresponding gas flow pattern across the matrix for a period can differ from the other flow pattern for the former or next period. Thus, the presence of the cracks makes the regenerator to operate from one period to the other period at different heat transfer performance. However, the performance ideally repeats after every complete cycle.

Most of the work reported in the literature on the leakages is related to rotary regenerators, as reported

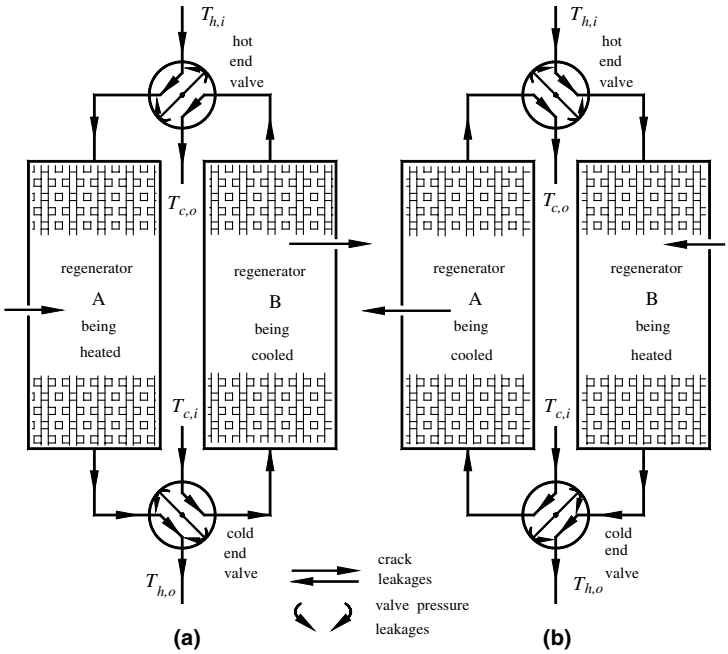

Fig. 1. A fixed-matrix regenerator with two matrices: (a) the present period (the matrix A being heated), and (b) the former period (the matrix A being cooled).

by Harper and Rohsenow [1], Banks and Ellul [2], Banks [3], Skiepko [4], Shah and Skiepko [5]. A few authors [6,7] discussed practical problems with regenerators in glass industry with the emphasis on the detrimental influence of leakages on the operation of fixed matrix regenerators. However, they did not provide any mathematical modeling or analysis of the leakages. Also, the problem of leakage of the cold air into or out of cracks of the matrices has not been taken into account in any existing mathematical models of heat transfer processes for the regenerators. Moreover, replacement of old checkerwork with new advanced specially designed regenerator packing may not provide the expected savings if it is not accompanied by an adequate sealing of the outer surface of the regenerator chamber.

For fixed-matrix regenerators, a methodology to investigate the effect of leakages on the regenerator heat transfer performance has been outlined by Shah and Skiepko [8]. The model, involving all categories of leakages, combines gas flow and leakage network modeling with heat transfer and pressure drop modeling. The objectives of this paper are as follows.

- Present comprehensive modeling for pressure and carryover leakages by coupling the leakage modeling, heat transfer modeling and pressure drop modeling for design and analysis methodology for fixed matrix regenerators.
- Outline quantitative effects of pressure leakages on heat transfer performance of fixed matrix regenerators since no such results are reported in the literature.

2. Modeling and governing equations

This section is aimed to describe a general overview of the modeling presented by Shah and Skiepko [8]. The regenerator consists of an internal regenerator and an actual regenerator as shown in Fig. 2. The internal regenerator consists of matrices, and the actual regenerator consists of the internal regenerator, housing and valves. The pressure leakages through the valves as well as the carryover leakages occur outside the internal regenerator and within the boundaries of the actual regenerator. However, the crack leakages refer to the internal regenerator because they are due to some cracks occurring in the housing of the matrices caused by thermal stresses during operation at high temperatures. Since the cracks can be located differently along the height of each matrix, the output system parameters of the two matrices can be different during two neighbouring periods. In turn, modeling of transport processes with the cracks present must couple two consecutive periods. Both together constitute a complete repeatable cycle (a total period) in operation for each matrix. Then, we need to consider energy transfer for the present and former periods for each matrix, as shown in Fig. 2,

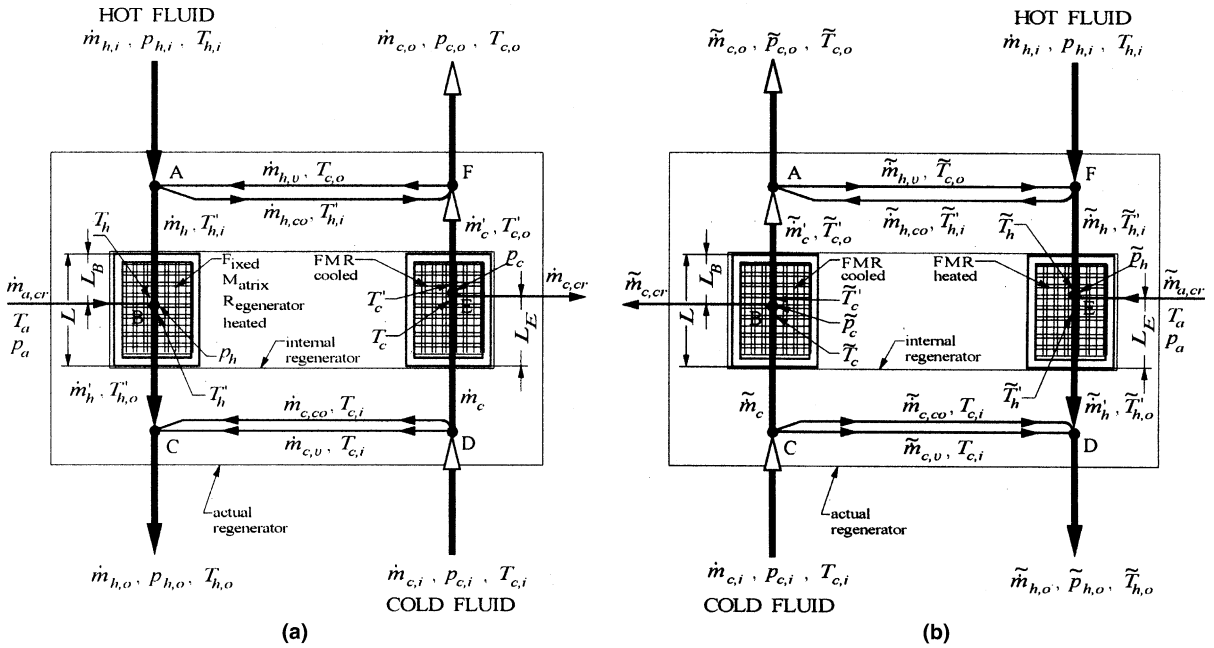

Fig. 2. The fixed-matrix regenerator gas flow network model with all categories of leakages: (a) the present period, (b) the former period.

linking the parameters via the effectiveness. The modeling is based on following idealizations:

(a) The regenerator operates under regular periodic conditions featured by repeatability of quantitative properties of the transfer process in alternate periods.
(b) Gas flow across the matrix flow area is uniform and has mass flow rate constant at the inlet as well as constant inlet temperature.
(c) The thermophysical properties of both fluids and matrix wall material are assumed constant as well as heat transfer coefficients throughout the whole matrix or selected parts of it during respective periods; the values for the heating period can differ from those for the cooling period.
(d) Longitudinal heat conduction in the wall and the fluids is negligible.
(e) The transverse conduction in the matrix in the wall thickness direction is included into considerations by incorporating the heat conduction resistance within the wall into an bulk heat transfer coeffcient.
(f) The mass and geometrical properties of the matrix are spatially uniform.
(g) The time required to switch the regenerator from one period to another is negligible compared to either hot or cold gas flow period.
(h) All gas streams flowing across the regenerator behave as mixtures of ideal gases and can reach equilibrium instantaneously when they are mixed.
(i) Heat losses from the regenerator housing to the surroundings are negligible.

Output results of the regenerator analysis performed based on the above idealizations are valid provided that transient processes occurring after the switching moment affect the regenerator operation insignificantly. Hence, the regenerator effectiveness is defined based on temperatures averaged over relevant periods. Also, all properties should be considered as averaged in the same manner.

2.1. Modeling of actual regenerator with leakages

It can be seen in Fig. 2a and b that all the leakages (apart from those through the cracks) are located within the region bounded between the internal regenerator (represented by the matrices), and an actual regenerator considered as the internal regenerator with its housing and valves. Consequently, transport processes within an actual regenerator can be regarded as coupling of the following phenomena:

(a) heat transfer, fluid flow and pressure drop across the internal regenerator affected by crack leakages,
(b) gas leakages through the regenerator valves and carryover transport,
(c) mixing resulting from leakages within the region between boundaries of the actual and internal regenerators as well as at the cracks.

For a complete modeling, we have to combine two gas flow patterns in the regenerator, referred to present and former periods, as shown in Fig. 2. To construct a model of the regenerator with leakages, all leakage flow rates shown in Fig. 2 should be expressed with pertinent equations. In addition, mass and energy balances at the mixing points A, B, ..., F in Fig. 2a and b will also be a part of the modeling, where appropriate. Note also that by virtue of idealization (h) mentioned earlier, stream mixing processes and energy interchanges associated with are described here by balances formulated based on classical thermodynamics. To consider gas–matrix radiation heat transfer in modeling, the exhaust gas (hot gas) is assumed to be a mixture of carbon dioxide and water vapor (also with nitrogen and oxygen). On the contrary, the cold gas (moist air) practically neither emits nor absorbs of thermal radiation. The actual regenerator of Fig. 2a and b represents a total of 50 unknown flow rates and temperatures as listed in Table 1.

The equations available to determine these unknowns are:

Table 1
The unknowns for the actual regenerator

Description	Present period, see also in Fig. 2a	Former period, see also in Fig. 2b
Valve pressure leakages	$\dot{m}_{c,\upsilon}$, $\dot{m}_{h,\upsilon}$	$\tilde{\dot{m}}_{c,\upsilon}$, $\tilde{\dot{m}}_{h,\upsilon}$
Carryover leakages	$\dot{m}_{c,co}$, $\dot{m}_{h,co}$	$\tilde{\dot{m}}_{c,co}$, $\tilde{\dot{m}}_{h,co}$
Mass flows between actual and internal regenerators:		
(a) before the crack		
• cold gas	$\dot{m}_c$	$\tilde{\dot{m}}_c$
• hot gas components, where $j = CO_2$, H_2O, N_2, O_2	$\dot{m}_{h,j}$	$\tilde{\dot{m}}_{h,j}$
(b) after the crack		
• cold gas	$\dot{m}'_c$	$\tilde{\dot{m}}'_c$
• hot gas components, where $j = CO_2$, H_2O, N_2, O_2	$\dot{m}'_{h,j}$	$\tilde{\dot{m}}'_{h,j}$
Mass flow rates at the outlets of the actual regenerator:		
• cold gas components	$\dot{m}_{c,o,j}$	$\tilde{\dot{m}}_{c,o,j}$
• hot gas components, where $j = CO_2$, H_2O, N_2, O_2	$\dot{m}_{h,o,j}$	$\tilde{\dot{m}}_{h,o,j}$
Gas temperatures from the actual regenerator to:		
• outside	$T_{c,o}$, $T_{h,o}$	$\widetilde{T}_{c,o}$, $\widetilde{T}_{h,o}$
• internal regenerator	$T'_{h,i}$	$\widetilde{T}'_{h,i}$
Number of unknowns	25	25
Total		50

- pressure leakages in valves (four equations),
- carryover leakage flows (four equations),
- mass flow rate balances at junction points (26 equations),
- energy balances at junction points (six equations).

Therefore, as shown in details in Table 2, there are a total of 40 linear/nonlinear equations available to determine 50 unknowns of the actual regenerator. Thus, to get the equation system closed, a model of the internal regenerator must provide the needed 10 equations for some 10 unknowns given in Table 1.

2.2. Modeling of internal regenerator

In order to investigate the influence of leakages on regenerator heat transfer performance, we combine modeling of the actual regenerator with leakages and that of internal regenerator matrices with heat transfer and pressure drop modeling. Note that the crack leakages affect the performance of the internal regenerator. Thus, they should be involved into the model. For this purpose, we divide each matrix into two parts, above and below an idealized point where the crack leakage enters into and exits from the matrix, i.e., points B and E in Fig. 2. Such idealized models of the internal regenerator are presented in Fig. 3.

Now let us discuss the modeling approach followed by the list of equations for the analysis. For the present period, at point B in the left matrix of Fig. 3a, a mixing process occurs between the ambient air leaking in through the cracks and hot gas stream coming down from the upper part of the matrix. At point E in the right matrix, the cold gas stream flowing up from the lower part is split into the remaining cold gas stream flowing to the upper part of the matrix and the leakage to the ambient through the cracks. For the former period, Fig. 3b, mixing of the streams occurs at point E and splitting of cold gas occurs at point B. Thus, we idealize this modeling with only one horizontal plane identified by one point in each of the two matrices where the gas leakages to or from ambient take place; no leakages take place within individual half matrices above or below the planes going through points B and E on the hot and cold gas sides of the internal regenerator. Then, to take into account the effect of crack leakages, we divide each matrix into two parts, above and below a horizontal plane where the crack leakage enters into and exits from the matrix, i.e., horizontal planes through points B and E in Fig. 3. In turn, the left matrix consists of two parts of heights L_B and $L - L_B$ separated at point B between them—see in Fig. 3. Similarly, the right matrix is disjoined at point E into two parts of heights L_E and $L - L_E$. Now, because there are no leakages within individual split matrices, each split matrix of the internal regenerator can be modelled as a separate sub-regenerator

Table 2
Model equations for the actual regenerator

Equations for the present period, see also in Fig. 2a	Equations for the former period, see also in Fig. 2b
Pressure leakages mass flow rates	
$\dot{m}_{c,\upsilon} = C_d \cdot A_{c,\upsilon} \cdot \sqrt{2 \cdot \rho_{c,i} \cdot (p_{c,i} - p_{h,o})}$	$\tilde{\dot{m}}_{c,\upsilon} = C_d \cdot A_{c,\upsilon} \cdot \sqrt{2 \cdot \rho_{c,i} \cdot (p_{c,i} - \tilde{p}_{h,o})}$
$\dot{m}_{h,\upsilon} = C_d \cdot A_{h,\upsilon} \cdot \sqrt{2 \cdot \rho_{c,o} \cdot (p_{c,o} - p_{h,i})}$	$\tilde{\dot{m}}_{h,\upsilon} = C_d \cdot A_{h,\upsilon} \cdot \sqrt{2 \cdot \tilde{\rho}_{c,o} \cdot (\tilde{p}_{c,o} - p_{h,i})}$
Carryover leakages mass flow rates	
$\dot{m}_{c,co} = \frac{A_{fr}}{P_c} \cdot \left[\sum_{n=1}^{N} (L_n \cdot \sigma_n \cdot \tilde{\rho}_{c,n}^{(av)}) + \frac{\Delta V \cdot \rho_{c,i}}{A_{fr}} \right]$	$\tilde{\dot{m}}_{c,co} = \frac{A_{fr}}{P_c} \cdot \left[\sum_{n=1}^{N} (L_n \cdot \sigma_n \cdot \rho_{c,n}^{(av)}) + \frac{\Delta V \cdot \rho_{c,i}}{A_{fr}} \right]$
$\dot{m}_{h,co} = \frac{A_{fr}}{P_h} \cdot \left[\sum_{n=1}^{N} (L_n \cdot \sigma_n \cdot \tilde{\rho}_{h,n}^{(av)}) + \frac{\Delta V \cdot \tilde{\rho}'_{h,o}}{A_{fr}} \right]$	$\tilde{\dot{m}}_{h,co} = \frac{A_{fr}}{P_h} \cdot \left[\sum_{n=1}^{N} (L_n \cdot \sigma_n \cdot \rho_{h,n}^{(av)}) + \frac{\Delta V \cdot \rho'_{h,o}}{A_{fr}} \right]$
Mass flow rate balances at junction points	
Point A:	Point A:
$\dot{m}_{h,j} + \dot{m}_{h,co,j} - \dot{m}_{h,\upsilon} \cdot f_{c,o,j} - \dot{m}_{h,i} \cdot f_{h,i,j} = 0$	$\tilde{\dot{m}}_{c,o,CO_2} + \tilde{\dot{m}}_{h,\upsilon} \cdot \tilde{f}_{c,o,CO_2} - \tilde{\dot{m}}_{h,co} \cdot \tilde{f}'_{h,CO_2} = 0$
where $j = CO_2$, H_2O, N_2, O_2	$\tilde{\dot{m}}_{c,o,j} - \tilde{\dot{m}}'_c \cdot \tilde{f}_{c,i,j} + \tilde{\dot{m}}_{h,\upsilon} \cdot \tilde{f}_{c,o,j} - \tilde{\dot{m}}_{h,co} \cdot \tilde{f}'_{h,j} = 0$
	where $j = H_2O$, N_2, O_2
Point C:	Point C:
$\dot{m}_{h,o,CO_2} = \dot{m}'_{h,CO_2}$	$\tilde{\dot{m}}_c + \tilde{\dot{m}}_{c,\upsilon} + \tilde{\dot{m}}_{c,co} - \dot{m}_{c,i} = 0$
$\dot{m}_{h,o,j} - \dot{m}'_{h,j} - (\dot{m}_{c,\upsilon} + \dot{m}_{c,co}) \cdot f_{c,i,j} = 0$	
where $j = H_2O$, N_2, O_2	
Point D:	Point D:
$\dot{m}_c + \dot{m}_{c,\upsilon} + \dot{m}_{c,co} - \dot{m}_{c,i} = 0$	$\tilde{\dot{m}}_{h,o,CO_2} = \tilde{\dot{m}}'_{h,CO_2}$
	$\tilde{\dot{m}}_{h,o,j} - \tilde{\dot{m}}'_{h,j} - (\tilde{\dot{m}}_{c,\upsilon} + \tilde{\dot{m}}_{c,co}) \cdot f_{c,i,j} = 0$
	where $j = H_2O$, N_2, O_2
Point F:	Point F:
$\dot{m}_{c,o,CO_2} + \dot{m}_{h,\upsilon} \cdot f_{c,o,CO_2} - \dot{m}_{h,co} \cdot f'_{h,CO_2} = 0$	$\tilde{\dot{m}}_{h,j} + \tilde{\dot{m}}_{h,co,j} - \tilde{\dot{m}}_{h,\upsilon} \cdot \tilde{f}_{c,o,j} - \dot{m}_{h,i} \cdot f_{h,i,j} = 0$
$\dot{m}_{c,o,j} + \dot{m}_{h,\upsilon} \cdot f_{c,o,j} - \dot{m}_{h,co} \cdot f'_{h,j} - \dot{m}'_c \cdot f_{c,i,j} = 0$	where $j = CO_2$, H_2O, N_2, O_2
where $j = H_2O$, N_2, O_2	
Energy balances at junction points	
Point A:	Point A:
$\sum_j (\dot{m}_h \cdot H'_{h,i})_j + \dot{m}_{h,co} \cdot \sum_j (f'_h \cdot H'_{h,i})_j + -\dot{m}_{h,\upsilon} \cdot \sum_j (f_{c,o} \cdot H_{c,o})_j +$	$\sum_j (\tilde{\dot{m}}_{c,o} \cdot \tilde{H}_{c,o})_j + \tilde{\dot{m}}_{h,\upsilon} \cdot \sum_j (\tilde{f}_{c,o} \cdot \tilde{H}_{c,o})_j +$
$- \dot{m}_{h,i} \cdot \sum_j (f_{h,i} \cdot H_{h,i})_j = 0$	$- \tilde{\dot{m}}_{h,co} \cdot \sum_j (\tilde{f}'_h \cdot \tilde{H}'_{h,i})_j - \tilde{\dot{m}}'_c \cdot \tilde{H}'_c = 0$
Point C:	Point D:
$\sum_j (\dot{m}_{h,o} \cdot H_{h,o})_j - \sum_j (\dot{m}'_h \cdot H'_{h,o})_j + -(\dot{m}_{c,\upsilon} + \dot{m}_{c,co}) H_{c,i} = 0$	$\sum_j (\tilde{\dot{m}}_{h,o} \cdot \tilde{H}_{h,o})_j - \sum_j (\tilde{\dot{m}}'_h \cdot \tilde{H}'_{h,o})_j + -(\tilde{\dot{m}}_{c,\upsilon} + \tilde{\dot{m}}_{c,co}) H_{c,i} = 0$
Point F:	Point F:
$\sum_j (\dot{m}_{c,o} \cdot H_{c,o})_j + \dot{m}_{h,\upsilon} \cdot \sum_j (f_{c,o} \cdot H_{c,o})_j +$	$\sum_j (\tilde{\dot{m}}_h \cdot \tilde{H}'_{h,i})_j + \tilde{\dot{m}}_{h,co} \cdot \sum_j (\tilde{f}'_h \cdot \tilde{H}'_{h,i})_j +$
$- \dot{m}_{h,co} \cdot \sum_j (f'_h \cdot H'_{h,i})_j - \dot{m}'_c \cdot H'_c = 0$	$- \tilde{\dot{m}}_{h,\upsilon} \cdot \sum_j (\tilde{f}_{c,o} \cdot \tilde{H}_{c,o})_j + -\dot{m}_{h,i} \cdot \sum_j (f_{h,i} \cdot H_{h,i})_j = 0$
where $j = CO_2$, H_2O, N_2,O_2	where $j = CO_2$, H_2O, N_2,O_2
Number of equations for present period: 20	Number of equations for former period: 20
Total number of equations: 40	

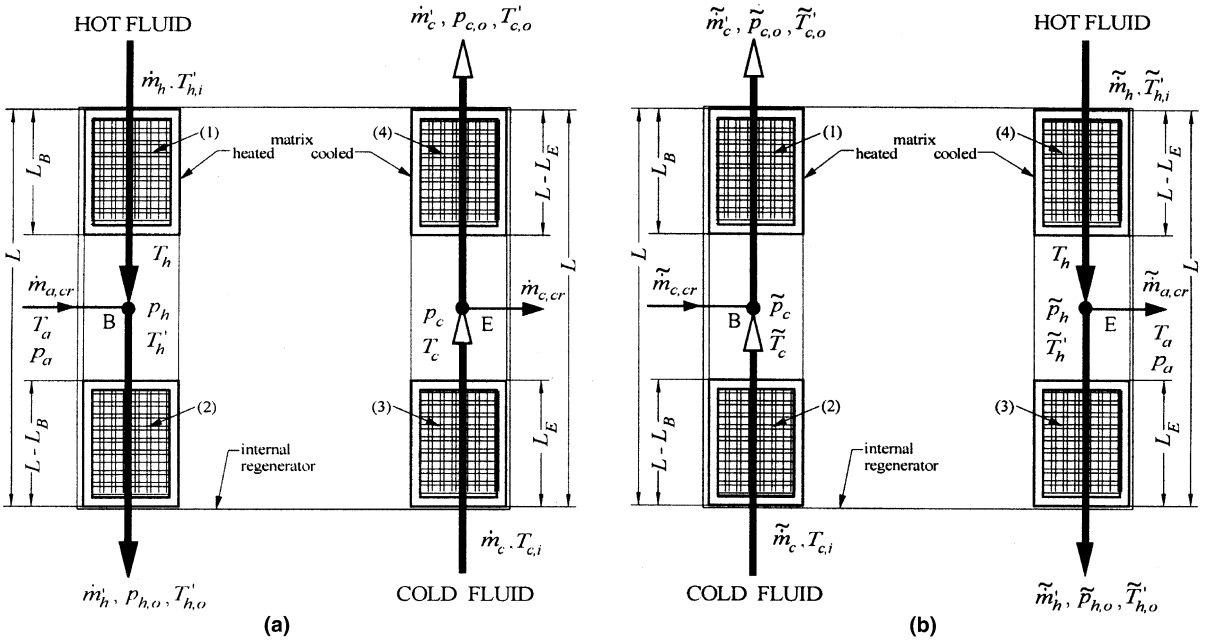

Fig. 3. A model of the internal regenerator with crack leakages: (a) the network model of the present period of Fig. 2a; (b) the network model of the former period of Fig. 2b. Note that the symbol ~ is used to denote quantities referred to the former period and (1),...,(4) are particular parts of the internal regenerator (see also in Table 3).

using the conventional definition of the regenerator effectiveness since no leakages take place within individual half matrices. Based on the published design theory [9,10], description of the modeling applied to sub-regenerators of the internal regenerator is presented in Appendix A. The unknowns for internal modeling are presented in Table 3. The equations available for these unknowns are:

- crack pressure leakage mass flow rates (four equations),
- definition of effectiveness for particular parts (eight equations),
- outlet pressures from particular parts of the matrices (eight equations),
- mass balances at junction points (10 equations),
- energy balances at junction points (four equations),
- ε—NTU relations for particular parts (four equations).

These equations for modeling of the internal regenerator are presented in Table 4.

Thus the modeling of actual and internal regenerators results in solving 40 + 38 coupled linear/nonlinear equations for 50 + 28 unknowns, as summarized in Tables 1–4. Consequently, the modeling is well closed.

Table 3
The unknowns for the internal regenerators

Description	Present period see also in Fig. 3a	Former period see also in Fig. 3b
Crack leakage flow rates	$\dot{m}_{c,cr}$, $\dot{m}_{a,cr}$	$\tilde{\dot{m}}_{c,cr}$, $\tilde{\dot{m}}_{a,cr}$
Outlet gas temperatures from particular parts	T_c, T_h, $T'_{c,o}$, $T'_{h,o}$	$\tilde{T}_c$, $\tilde{T}_h$, $\tilde{T}'_{c,o}$, $\tilde{T}'_{h,o}$
Outlet pressure from the particular parts	p_c, p_h, $p_{c,o}$, $p_{h,o}$	$\tilde{p}_c$, $\tilde{p}_h$, $\tilde{p}_{c,o}$, $\tilde{p}_{h,o}$
Gas temperatures at mixing points	*Point B:* T'_h	*Point B:* $\tilde{T}'_c$
	Point E: T'_c	*Point E:* $\tilde{T}'_h$
Heat transfer effectivenesses indicated by superscripts (1), (2), (3) and (4) in the counter clockwise direction for particular parts of the internal regenerator shown in Fig. 3a and b:	left upper part $\varepsilon_i^{(1)}$; left lower part $\varepsilon_i^{(2)}$ right lower part $\varepsilon_i^{(3)}$; right upper part $\varepsilon_i^{(4)}$	
Number of unknowns	28	

Table 4
Model equations for the internal regenerator

Description	Present period see also Fig. 3a	Former period see also in Fig. 3b
1. Crack leakage mass flow rates	$\dot{m}_{c,cr} = C_d \cdot A_{cr}^{(r)} \cdot \sqrt{2\rho_c \cdot (p_c - p_a)}$ $\dot{m}_{a,cr} = C_d \cdot A_{cr}^{(\ell)} \cdot \sqrt{2\rho_a \cdot (p_a - p_h)}$	$\tilde{\dot{m}}_{c,cr} = C_d \cdot A_{cr}^{(\ell)} \cdot \sqrt{2\tilde{\rho}_c \cdot (\tilde{p}_c - p_a)}$ $\tilde{\dot{m}}_{a,cr} = C_d \cdot A_{cr}^{(r)} \cdot \sqrt{2\rho_a \cdot (p_a - \tilde{p}_h)}$
2. Outlet gas temperatures from particular parts of the internal regenerators determined based on definitions of the effectivenesses indicated for particular parts, shown in Fig. 3a and b by superscripts (1), (2), (3) and (4) in the counter clockwise direction	$\varepsilon_i^{(1)} = \frac{C_h \cdot (T'_{h,i} - T_h)}{C_{min}^{(1)} \cdot (T'_{h,i} - \widetilde{T}'_c)}$ $\varepsilon_i^{(2)} = \frac{C'_h \cdot (T'_h - T'_{h,o})}{C_{min}^{(2)} \cdot (T'_h - T_{c,i})}$ $\varepsilon_i^{(3)} = \frac{C_c \cdot (T_c - T_{c,i})}{C_{min}^{(3)} \cdot (\widetilde{T}'_h - T_{c,i})}$ $\varepsilon_i^{(4)} = \frac{C'_c \cdot (T'_{c,o} - T'_c)}{C_{min}^{(4)} \cdot (\widetilde{T}'_{h,i} - T'_c)}$	$\varepsilon_i^{(1)} = \frac{\widetilde{C}'_c \cdot (\widetilde{T}'_{c,o} - \widetilde{T}'_c)}{C_{min}^{(1)} \cdot (T'_{h,i} - \widetilde{T}'_c)}$ $\varepsilon_i^{(2)} = \frac{\widetilde{C}_c \cdot (\widetilde{T}_c - T_{c,i})}{C_{min}^{(2)} \cdot (T'_h - T_{c,i})}$ $\varepsilon_i^{(3)} = \frac{\widetilde{C}'_h \cdot (\widetilde{T}'_h - \widetilde{T}'_{h,o})}{C_{min}^{(3)} \cdot (\widetilde{T}_h - T_{c,i})}$ $\varepsilon_i^{(4)} = \frac{\widetilde{C}_h \cdot (\widetilde{T}'_{h,i} - \widetilde{T}_h)}{C_{min}^{(4)} \cdot (\widetilde{T}'_{h,i} - T'_c)}$
3. Equations for outlet pressures: • outlet pressure from part (1) • outlet pressure from part (2) • outlet pressure from part (3) • outlet pressure from part (4)	 $p_h = p_{h,i} - \Delta p_h$ $p_{h,o} = p_h - \Delta p'_h$ $p_c = p_{c,i} - \Delta p_c$ $p_{c,o} = p_c - \Delta p'_c$	 $\tilde{p}_{c,o} = \tilde{p}_c - \Delta\tilde{p}'_c$ $\tilde{p}_c = p_{c,i} - \Delta\tilde{p}_c$ $\tilde{p}_{h,o} = \tilde{p}_h - \Delta\tilde{p}'_h$ $\tilde{p}_h = p_{h,i} - \Delta\tilde{p}_h$
4. Mass balances at junction points	Point B: $\dot{m}'_{h,CO_2} - \dot{m}_{h,CO_2} = 0$ $\dot{m}'_{h,j} - \dot{m}_{h,j} - \dot{m}_{a,cr} \cdot f_{a,j} = 0$ where $j = H_2O$, N_2, O_2 Point E: $\dot{m}'_c + \dot{m}_{c,cr} - \dot{m}_c = 0$	Point B: $\tilde{\dot{m}}'_c + \tilde{\dot{m}}_{c,cr} - \tilde{\dot{m}}_c = 0$ Point E: $\tilde{\dot{m}}'_{h,CO_2} - \tilde{\dot{m}}_{h,CO_2} = 0$ $\tilde{\dot{m}}'_{h,j} - \tilde{\dot{m}}_{h,j} - \tilde{\dot{m}}_{a,cr} \cdot f_{a,j} = 0$ where $j = CO_2$, H_2O, N_2, O_2
5. Energy balances at junction points	Point B: $\sum_j (\dot{m}'_h \cdot H'_h)_j - \sum_j (\dot{m}_h \cdot H_h)_j +$ $- \dot{m}_{a,cr} \cdot H_a = 0$ where $j = CO_2$, H_2O, N_2, O_2 Point E: $H'_c - H_c = 0$	Point B: $\widetilde{H}'_c - \widetilde{H}_c = 0$ Point E: $\sum_j (\tilde{\dot{m}}'_h \cdot \widetilde{H}'_h)_j - \sum_j (\tilde{\dot{m}}_h \cdot \widetilde{H}_h)_j +$ $- \tilde{\dot{m}}_{a,cr} \cdot H_a = 0$ where $j = CO_2$, H_2O, N_2, O_2
6. The effectiveness of particular parts $N = (1), (2), (3), (4)$ of the internal regenerators	$\varepsilon_i^{(N)} = \varepsilon_i^{(N)}[NTU_o^{(N)}, C^{*(N)}, C_r^{*(N)}]$ where $N = (1 =$ left upper corner), $(2 =$ left lower corner), $(3 =$ right lower corner), $(4 =$ right upper corner), see parts also in Fig. 3	
Total number of equations	38	

Since the exhaust gas (hot gas) is assumed to be a mixture of nitrogen, oxygen, carbon dioxide and water vapor, it is analysed with these gas components. Necessary mass balances of the components of gases have increased the number of equations/unknowns to be 78 compared to 52 as reported in [8] where the exhaust gas was considered as one component only. Note mass fractions are denoted by f with appropriate subscripts in Tables 2 and 4. They can be expressed by means of unknowns already specified and those referred to the inlets are known on input data. The same refers to heat capacity rates C, pressure drops Δp and NTU_o, C^* and C_r^* . The equations mentioned above should be supplemented with some empirical information referring to

discharge coefficients C_d for flow through valves and cracks as well as correlations describing heat transfer coefficients and friction factors for heat transfer and pressure drop modeling of the internal regenerator taking into account effects resulting from the crack leakages for the complete modeling. However, there are no data available for the coefficient of discharge C_d for gap (leakage) flow through the valve or for cracks in the housing. Thus, until better information is available, we assume $C_d = 0.80$ as an approximation. This approximation does not make conclusions invalid on leakage effects presented in this paper because these have been derived using specific values of the leakage factor. Note also that formulas describing crack leakages given in Table 4 are applicable to cracks of a large dimension and not applicable to small minute cracks. For small minute cracks through thick walls (for $Re < 1$ where only viscous and pressure forces are dominant), the well-known Darcy's law for viscous flow through porous media should be used. In that case, the permeability of the walls should be determined experimentally. Empirical correlations describing heat transfer coefficients and friction factors for pressure drop are presented in Appendix A.

The system of equations is strongly nonlinear due to nonlinear forms of the most equations as well as the inclusion of thermal radiation. We have used an iterative Newton–Raphson method [11] to solve this system, see details in Appendix B. A computer program has been written and thoroughly checked for convergence and accuracy.

3. Case study for leakage effects

The leakage effect presented in the paper has been evaluated by numerical experiments carried out for the rating problem using an assumed regenerator composed of two fixed matrices, as shown in Fig. 1. The regenerator is described below in terms of flow inlet data, matrix and gas properties, transfer coefficients and specific leakage paths taken into considerations.

3.1. Matrix properties and transfer coefficients

A single square chimney flue along the regenerator height, shown in Fig. 4, is constructed of parallelpiped checkers of $230 \times 114 \times 64$ mm. The checkers are made of ceramic material of AS type operating at temperature of 1350 °C. The regenerator operating conditions and characteristics are given in Table 5.

In order to assess the leakage effects, we have considered two modes of flue (hot) gas–matrix heat transfer: (1) convection only, and (2) convection and radiation combined while the cold gas (moist air) is heated by the matrix under convection mode only. The convection

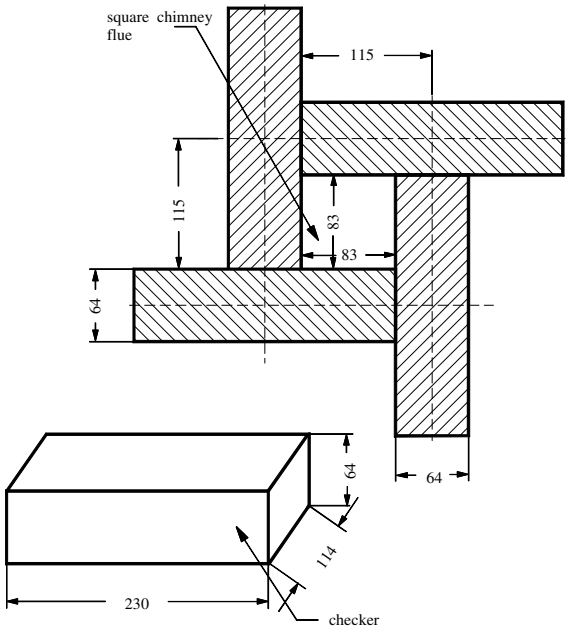

Fig. 4. Chimney flue and checker arrangement used for the case study. All dimensions are in mm.

heat transfer coefficient for either air/flue gas under flow along a flue is calculated using Böhm's correlation [12] summarized in Appendix A.2. The radiation heat transfer between the flue gas and the surface of the matrix, which is usually neglected in low temperature regenerator analysis, can become important for high temperature regenerators such as for glass or metal industry [13,14]. Thus, this mode of heat transfer is included in the analysis by a method [15] described in Appendix A.3. The transverse heat conduction in the matrix material is taken into considerations by the Hausen method [16]. The pressure drop analysis is straightforward [10], as summarized in Appendix A.4. Moreover, equations of state, data describing enthalpy, and thermophysical properties are introduced as well in computerized calculations; see the relevant information in Appendix A.5.

3.2. Leakage paths studied

Let us first describe the assumptions made for the leakage analysis followed by the description of the leakage paths. We idealize that the cold gas pressure is higher than the ambient pressure and hot gas pressure is lower than the ambient pressure. For all cases considered, we have kept for the present period constant pressure leakages of 5% and 10% of the cold gas mass flow rate at the regenerator inlet. In order to maintain these constant leakages, it is necessary to use specific values for leakage flow areas either in valves or in cracks as input data. For the former period of the regenerator

Table 5
Regenerator data used for the case study

Regenerator operating conditions		Regenerator characteristics	
Air inlet mass flow rate	$\dot{m}_{c,i} = 70$ kg/s	Flow arrangement	*Counterflow*
Air inlet temperature	$T_{c,i} = 90$ °C	Number of matrices	2
Air inlet gauge pressure	$p_{c,i} = 1000$ Pa	Length of periods	$P_h = P_c = 5400$ s
Air inlet humidity ratio	$x_{c,i} = 10$ g/kg	Single matrix frontal area	$A_{fr} = 40$ m^2
Ambient air temperature	$T_a = 20$ °C	Coverage factor for frontal area	$C_{fr} = 1$
Ambient air pressure	$p_a = 101325$ Pa	Matrix height	$L = 40$ m
Hot gas inlet mass flow rate	$\dot{m}_{h,i} = 70.0$ kg/s	Crack locations	$L_B = 10$ m, $L_E = 30$ m
Hot gas inlet temperature	$T_{h,i} = 1300$ °C	Volume between matrix and valve	$\Delta V = 1$ m^3
Hot gas inlet gauge pressure	$p_{h,i} = -500$ Pa	Valve/crack discharge coefficient	$C_d = 0.8$
Hot gas inlet composition by mass fractions:		Matrix porosity	$\sigma = 0.32$
Carbon dioxide	$f_{h,i,CO_2} = 25.55\%$	Matrix packing factor	$Y = 15.4$ m^2/m^3
Water vapor	$f_{h,i,H_2O} = 3.62\%$	Matrix hydraulic diameter	$D_h = 0.083$ m
Nitrogen	$f_{h,i,N_2} = 69.41\%$	Matrix material specific heat	$c_w = 1.0$ kJ/(kg K)
Oxygen	$f_{h,i,O_2} = 1.42\%$	Matrix material mass density	$\rho_w = 1950$ kg/m^3
Ash	$f_{h,i,ash} = 0.0\%$	Matrix material thermal conductivity	$\lambda_w = 1.4$ W/(m K)

operation, we assume that the same unsealed area exists for the leakage. However, due to different gas properties and gas pressure in matrix for the former and present periods, leakage through the same crack during the former period of operation is not the equal to that in the present period what is also included into the modelling. The following are the specific leakage paths considered as shown in Fig. 2a and b:

1. Pressure leakages in valves: (1a) For the present period, the leakage path is from the point D to C; and in turn, for the former period it is from C to D; (1b) For the present period, the leakage path is from the point F to A; and for the former period it is from A to F.
2. Pressure leakages across cracks: (2a) Across a crack at the plane of point B, the ambient air leaks in the left matrix during the present period; in turn, during the former period, the cold gas from the left matrix leaks to ambient across the same crack, while the housing for the right matrix is leak-free; (2b) Across a crack at the plane of point E, the cold gas leaks to the ambient during the present period; in turn, during the former period, the ambient air leaks into the right matrix across the same crack, while the housing for the left matrix is leak-free.
3. Combined case of pressure leakages: across a crack in the plane of point B, 5% ambient air leaks in the left matrix during the present period; and at the same time across a crack in the plane of point E, 5% cold gas leaks to the ambient. In addition; and at the same time, 5% cold gas leaks from point D to C in the cold end valve, and 5% cold fluid leaks from point F to A in the hot end valve. Under the former period the leakage flows are opposite in direction and due to different properties of leaking gases are also different in amounts.
4. For comparisons, the case of 0% pressure leakage has been calculated as a reference case. For all cases studied, the carryover leakages have been included into considerations.

4. Effect of leakages

In this section, we will provide numerical results for specific cases outlined in the preceding subsection. First, gas and leakage flow rates are presented and discussed. The effect of leakages on regenerator performance is summarized the next subsection.

4.1. Gas and leakage flow rates

In Fig. 5, gas and leakage flow rates are summarized using input data as for regenerator data under the case study. The flow rate results are juxtaposed horizontally and vertically such that two horizontal cases, when compared to each other, demonstrate the effect of leakages for a period under consideration—the left refers to case of 0% pressure leakage, the right refers to finite pressure leakages across valves and cracks. However, two vertical sets of results, for which leakage amount is held constant, show variation of the regenerator thermal fluid-flow parameters in two neighboring periods, upper for the present and lower for the former.

Now let us review the results. For 0% pressure leakage, variable flow rates are the mirror images for present and former periods as found from Fig. 5a and c. This due to the fact that the crack leakages are not present while both the matrices are the same operating during identical periods.. However, when the crack pressure leakages are present, the flow rates can be different for two neighboring periods as found from Fig. 5b and d;

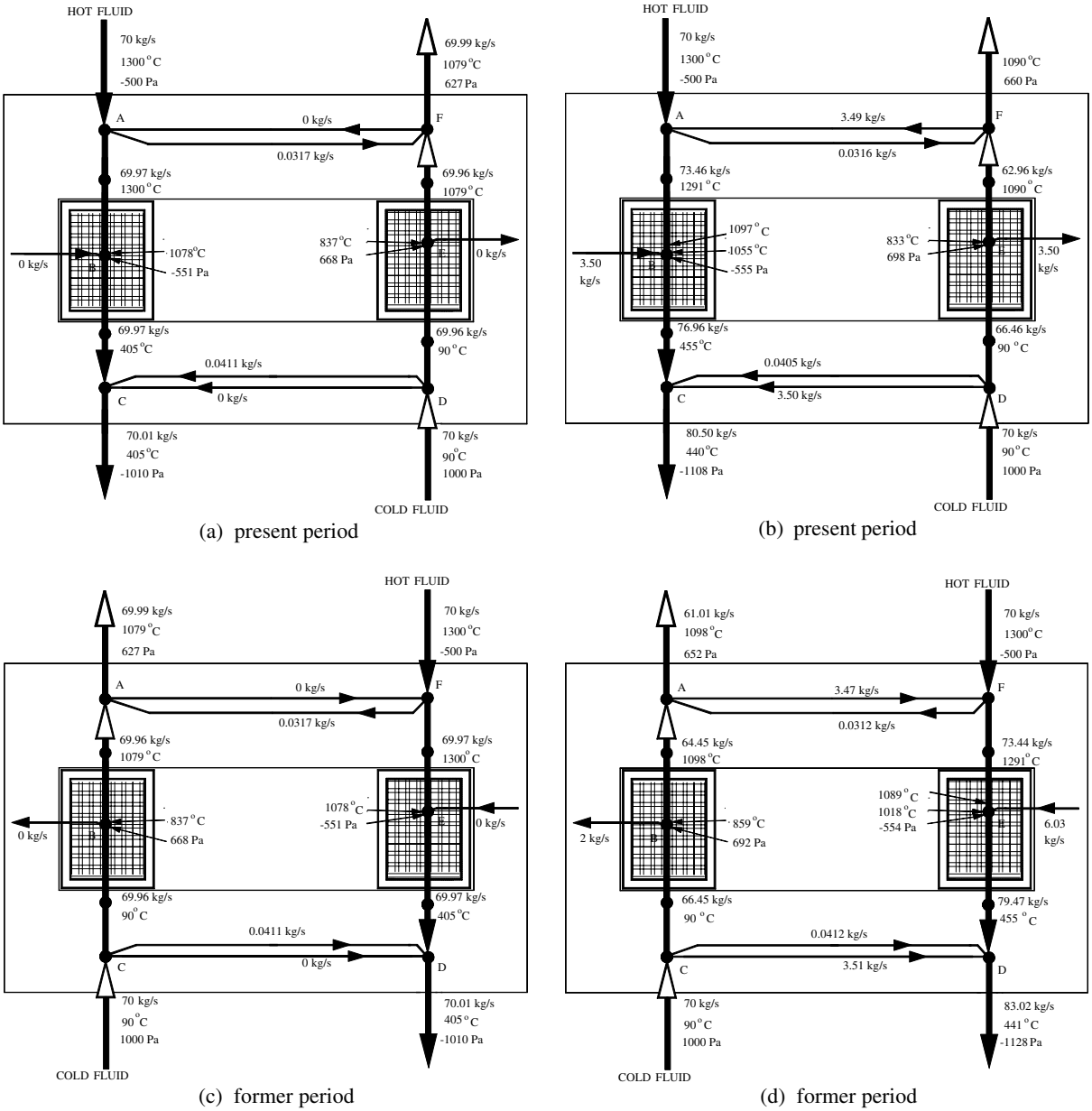

Fig. 5. Gas and leakage flow rates for the regenerator case study, convection and radiation transfer modes under consideration: (a) the case of 0% pressure leakage during the present period, (b) the case of finite pressure leakages across valves and cracks during the present period, (c) the case of 0% pressure leakage during the former period, (d) the case of finite pressure leakages across valves and cracks during the former period.

and in turn, the regenerator output parameters are different for the same leakage (crack) flow areas! To show this, the results presented in Fig. 5b were determined assuming specific flow areas for leakages such that all categories of crack and valve pressure leakages occur for the present period for 5% cold gas mass flow rate inflowing the matrix. Note in Fig. 5b that under the present period, the ambient air flows in the left matrix through a crack at point B and outflow of the heated gas takes place at crack E. In turn, to hold 5% leakage at either crack, the corresponding flow areas must be different for the left and right matrices. However, the former period (for which the crack flow areas remain unchanged) is featured by leaking out of the heated gas at crack B and leaking in the ambient air at crack E as shown in Fig. 5d. The mass density of the heated

gas leaking out at point B during the former period is much smaller than the mass density of the ambient air inflowing the left matrix during present period (because of their different mass densities due to a large difference in their temperatures, 859 °C vs. 20 °C). Thus through the same flow area only 2 kg/s of the heated gas can flow out the left matrix during the former period when compared to 3.5 kg/s of the ambient air flowing in the left matrix during the present period. However, at point E of the right matrix, the phenomenon is opposite: during the present period, the leakage out of the useful heated gas is 3.5 kg/s at 833 °C; during the former period (the flow area remains the same) the leakage inflow of ambient air at point E is about 6 kg/s due to much higher mass density of the ambient at 20 °C. The described variability in leakage amounts of the useful heated gas affects the actual regenerator effectiveness in such a manner that the effectiveness is lower for the present period than that for the former period due to smaller leakage and therefore higher mass flow rate of the useful heat gas at the regenerator outlet. Regarding the amounts of the crack leakages, the largest is inflow of ambient air into the hot gas; note that about 6 kg/s of the ambient air mass flow rate inflowing the right matrix at point E under the former period. The smallest is outflow of the useful heated gas into ambient across the crack through which the ambient air inflows the hot gas during preceding period; it is 2 kg/s of the mass flow rate at point B of the left matrix under former period. The amount of the valve pressure leakages during two neighboring period are insignificantly different, all ranging 3.47–3.51 kg/s, the most probably due to small differences in driving pressure drops as well as mass densities of the leaking gases under two neighboring periods.

The carryover leakages, due to long duration of the periods, affect the flow rates insignificantly as the related mass flow rates are essentially small, roughly 0.03–0.04 kg/s vs. 70 kg/s of the cold gas mass flow rate inflowing the regenerator. Note also different amounts of the cold and hot gas carryovers caused by different properties of the moist air (cold gas) when compared to the hot flue gas being a product of combustion.

4.2. Effect of leakages on regenerator performance

We investigate the significance of the leakages by comparing the regenerator performance in terms of heat transfer effectiveness ε_b of the actual regenerator with some specific leakages, as specified in the preceding subsection. The actual regenerator effectiveness ε_b has been defined with details in [5], as

$$\varepsilon_b = \frac{Q_u}{Q_{max}} = \frac{\dot{m}_{c,o} \cdot (H_{c,o} - H_{c,i})}{C_{min} \cdot (T_{h,i} - T_{c,i})} \quad (1)$$

for both present and former periods, where Q_u represents amount of heat transferred per period to heated useful gas at its mass flow rate available, after deduction of all leakages, at the regenerator outlet; and Q_{max} is the maximum possible amount of heat transferred per period to useful heated gas at its inlet mass flow rate. The results presented refer to the percentage drop in actual heat transfer effectiveness ε_b. It is defined as the just difference between ε_b (%) for 0% pressure leakage (no leaks through valves and cracks, only carryover transport of both fluids occurs) and ε_b (%) at finite pressure leakage (under present period: 5% and 10% or 5% each individual for the combined case, as described in Section 3. Note also that the percentage values of pressure leakages mean ratios of leakage mass flow rate, where appropriate, to cold gas mass flow rate at the inlet to regenerator.

4.3. Convection transfer mode

The percentage drop in ε_b as a function of pressure leakage rate is shown in Fig. 6 for various leakage flow paths. It can be seen from Fig. 6 that the drop in ε_b depends approximately linearly on the amount of the pressure leakage. However, the quantitative effect is significantly dependent on where the leakage takes place. Thus, the results for valve leakages can be summarized with increasing significance for the effectiveness, as follows:

- The drop in the effectiveness due to leakage of the inlet cold gas through the leaking valve into the hot gas at the regenerator outlet (from point D to C and vice versa—see Fig. 2) is the lowest. The drop in the effectiveness is about 1.8% at 5% leakage and 3.8% at 10% leakage, which translates into about 0.4% drop per 1% such leakage for either period.

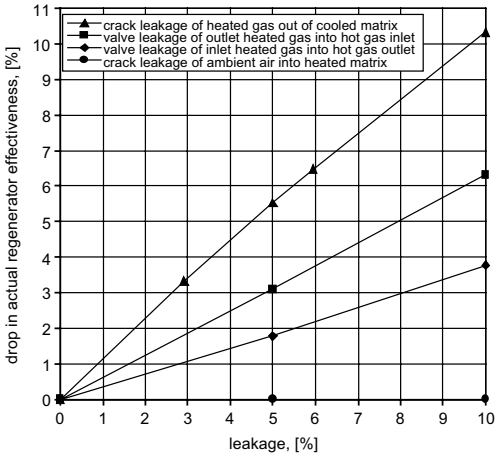

Fig. 6. The effect of pressure leakages on the actual regenerator effectiveness for convection heat transfer mode.

- When the heated cold gas leaks at the actual regenerator outlet (from point F to A and vice versa in Fig. 2) through the leaking valve into the hot gas inflowing the regenerator, the drop in the effectiveness is higher than that for the former case. It is about 3.1% at 5% leakage and 6.3% at 10% leakage, which yields 0.6% drop in the effectiveness per 1% such leakage for either period. Such higher detrimental effect for this case (when compared to the former case) is due to loss not only of the outlet useful cold gas mass flow rate caused by the leakage but also due to loss of some thermal energy because the leaking useful gas (after mixing with the hot gas) leaves the regenerator at the hot gas outlet temperature.

A more complex picture of the leakage effects is present when cracks appear across the matrix housing. For such cases, there is a significant difference in the drop for two neighboring periods as in Fig. 6. In particular, the results are as follows:

- For a period when the heated useful cold gas leaks across the cracked matrix into the ambient (the right matrix during present period in Fig. 2a or the left matrix during former period in Fig. 2b), the drop in the effectiveness of the actual regenerator for the corresponding period is quite significant, 5.5% at 5% leakage and 10.3% at 10% leakage; this results in drop in the effectiveness about 1% per 1% of the leakage. Such high drop in the effectiveness for this case when compared to the former cases is due to loss of thermal energy and mass flow rate with the crack leaking because the useful cold gas runs out to the ambient at very high temperature close to the outlet temperature.
- If there is a crack in housing of the matrix being heated (see the left matrix in Fig. 2a or the right matrix in Fig. 2b), the drop in the effectiveness of the actual regenerator for the corresponding period when the hot gas flows through the cracked matrix is negligibly small because the other matrix where the useful gas is heated up remains intact without any cracks.

In summary, the leakage through cracks have the most detrimental effect on the actual regenerator effectiveness when the useful gas leaks out of the matrix in which the cold gas is being heated. Pressure leakages in the valves either at the cold or hot end have a negligible impact on the effectiveness of the actual regenerator.

4.4. Convection and radiation transfer modes combined

Results obtained for this case are displayed in Fig. 7 where it can be observed similar qualitative trends in drop in the actual regenerator effectiveness due to pressure leakages as shown in Fig. 6 for the convection mode. Again, the cracks have most drop in the actual regenerator effectiveness.

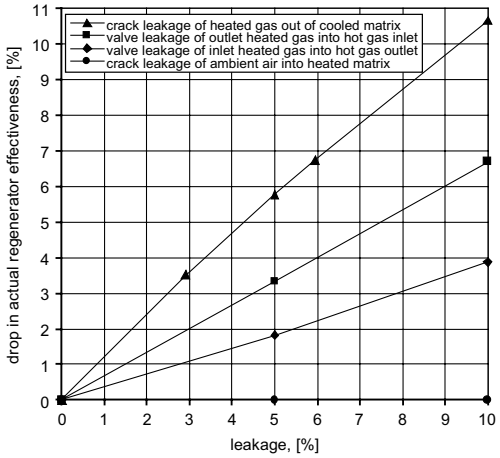

Fig. 7. The effect of pressure leakages on the actual regenerator effectiveness for convection and radiation heat transfer modes combined.

A comparison of the results in Figs. 6 and 7 indicate that the quantitative effect of pressure leakages on ε_b is only a small fraction higher when compared to those for the convection mode. If the heated gas leaks to the ambient (Fig. 2) through a crack in the regenerator housing, then such leakage results in the most drop in the actual regenerator effectiveness by about 1.1% per 1% of such leakage. The other leakages result in the drop in ε_b the same as it is for the convection mode. Thus due to the presence of radiation over the convection mode, the effect of the pressure leakages in ranges 0–10% is negligible for the actual regenerator effectiveness.

4.5. Combined pressure leakage effects

Now we consider the most general case of all categories of pressure leakages occurring simultaneously during the present period: (a) 5% ambient air leaks in the left matrix through a crack at point B; (b) 5% heated cold gas leaks to the ambient through a crack at point E; (c) 5% cold fluid leaks from point D to C in the cold end valve, (d) 5% cold fluid leaks from point F to A in the hot end valve. Leakages during the former period of the regenerator operation are determined based on equation system modeling of the actual and internal regenerators keeping the same magnitudes of leaking areas for leakage flows as for the present period. The results shown in Section 4.2 showed that when the radiation mode accompanies convection heat transfer, the difference in the leakage

effect is negligibly small. Therefore, the combined case is studied only for the convection mode. Moreover, the detrimental effect of various pressure leakages when expressed per 1% leakage is about the same for 5% and 10% leakages. Therefore, the combined case is studied for 5% each individual leakages (at the cold and hot end valves and through cracks), so that the total leakage during the present period is 15% of the cold gas that leaking into the hot gas and ambient, and 5% of the ambient air leaks into the hot gas. The drop in ε_b for this case is 10.8% for the present period and 8.5% for the former period; alternatively, it is 0.7% drop in the actual regenerator effectiveness per 1% of the total cold gas leakage.

5. Concluding remarks

The scope of the paper refers to the modeling and effect of the following leakages on regenerator performance: the pressure leakages through the regenerator valves and cracks in the housing and carryover leakages due to displacement of gas trapped into the void volumes of the matrices and headers (ducts). The system considered consists of two fixed matrix regenerators operating parallel but out of phase by one period. Modeling of such a system is based on a gas flow network in which the mass and energy balances along with the modeling of pressure and carryover leakages result in 78 equations coupled in a nonlinear system. The solution to these equations then provided quantitative gas and leakage flow rates based on which the effect of these leakages on the regenerator performance has been evaluated. The following are specific conclusions from the results obtained in this study.

- The deterioration in the performance due to leakages depends approximately linearly with the amount of leakage and varies significantly on the individual leakage path location.
- For valve leakages, the worst deterioration in ε_b results for leakage of the outlet heated gas into the waste hot gas at the regenerator inlet. Here the estimated deterioration in the effectiveness is ~0.6% per 1% such leakage. The valve leakage of the fresh cold gas into the hot gas leaving the regenerator provides the lowest drop in the actual regenerator effectiveness estimated at ~0.4% per 1% such leakage.
- The effect of the leakage through a crack in housing of an individual regenerator matrix is different for two neighboring periods. If the cracked housing surrounds a matrix being cooled the deterioration in the useful heat rate and actual regenerator effectiveness is the biggest for the period under considerations to be about ~1% per 1% of the leakage. If there is a crack in the regenerator housing of the matrix being heated, the drop in the useful heat rate and actual regenerator effectiveness is negligibly small for the period under study.
- For a combined case when all categories of leakages occur simultaneously, the resultant effect when expressed per 1% of the total cold gas leakage is ~0.7% drop in the actual regenerator effectiveness for either period.
- Worthy to mention is that the presence of radiation over the convection mode results in negligible drop in actual regenerator effectiveness.

Appendix A. Basic formulae for regenerator heat transfer effectiveness, heat transfer coefficients and pressure drop analysis

A.1. Regenerator heat transfer effectiveness

The regenerator effectiveness is calculated from the following expression that includes the effect of rotation and transverse conduction. For details on the derivation and explanation, refer to Shah and Sekulic [10].

$$\varepsilon = \frac{1-\exp\{\varepsilon_m \cdot (C^{*2}-1)/[2\cdot C^*(1-\varepsilon_m)]\}}{1-C^*\cdot\exp\{\varepsilon_m\cdot(C^{*2}-1)/[2\cdot C^*(1-\varepsilon_m)]\}}$$

where C^* and ε_m are given by

$$C^* = C_{min}/C_{max}$$

where

$$C_{min} = \min(C_h, C_c) \quad \text{and} \quad C_{max} = \max(C_h, C_c)$$

$$\varepsilon_m = C_{corr}\cdot\frac{NTU_{o,m}}{1+NTU_{o,m}}$$

$$C_{corr} = 1.0 - \frac{1}{9.0\cdot\left(C^*_{r,m}\right)^{1.93}}$$

$$C^*_{r,m} = 2\cdot C^*_r\cdot C^*/(1+C^*)$$

$$C^*_r = C_r/C_{min}$$

where

$$C_r = 2\cdot A_{fr}\cdot L\cdot\rho_w\cdot(1-\sigma)\cdot c_w/P_{tot}$$

$$NTU_{o,m} = 2\cdot NTU_o\cdot C^*/(1+C^*)$$

$$NTU_o = \frac{1}{[1/(h_h\cdot A_h)+R_w+1/(h_c\cdot A_c)]\cdot C_{min}}$$

$$R_w = r_w\cdot[(1/A_h)+(1/A_c)] \quad r_w = \delta\cdot\varphi^*/(3\cdot\lambda_w)$$

$$\varphi^* = 2.142\cdot(0.3+2.0\cdot Z)^{-0.5} \quad \text{for } Z \geqslant 5$$

$$\varphi^* = 1 - Z/15 \quad \text{for } Z \leqslant 5$$

$$Z = \delta^2 \cdot [(1/P_h) + (1/P_c)]/a \quad \text{where } a = \lambda_w(\rho_w \cdot c_w)$$

A.2. Convection heat transfer coefficient

The convection heat transfer coefficient for either air/flue gas turbulent flow along a flue is calculated from B(o)hm's formula [12] given by

$$h_C = 0.687 \cdot \frac{T_f^{0.25} \cdot G_{fr}^{0.8}}{D_h^{0.33} \cdot \rho_f^{0.80}} \tag{A.1}$$

where h_C [W/(m^2 K)], T_f [K], G_{fr} [kg/(m^2 s)], D_h [m] and ρ_f [kg/m^3] are: the convection heat transfer coefficient, flue gas temperature, mass velocity to be determined based on the frontal area, hydraulic diameter of the flow passages and gas mass density, respectively.

A.3. Radiation heat transfer coefficient

For the case study presented in the paper, the hot gas assumed contains heteropolar gases such as CO_2 and H_2O that can emit and absorb thermal radiation. Thus, the radiative heat transfer between the flue gas and the surface of the matrix is included in the analysis by the radiant heat transfer coefficient h_R defined by [13]

$$q_R = h_R \cdot (T_f - T_w) \tag{A.2}$$

where q_R is the net heat flux exchanged between the gas and matrix surface due to gas–matrix surface thermal radiation as a result of the temperature difference $T_f - T_w$. To calculate coefficient h_R we apply a method presented in [15] see also in [17] commonly used for thermal design of boilers. Hence, for the case when the flue gas does not have suspended solid particles one can find in [15] a formula

$$h_R = 5.670 \cdot 10^{-8} \cdot \frac{\in_w + 1}{2} \cdot \in_f \cdot T_f^3 \cdot \frac{1 - (T_w/T_f)^{3.6}}{1 - (T_w/T_f)} \tag{A.3}$$

where the emissivity of the matrix element surface is used to be $\in_w = 0.8$. Regarding the emissivity of the flue gas being of a mixture of CO_2, H_2O, N_2 and O_2 gases, the method [15,17] uses Hottel's data [18] correlated in [19] to describe by the following equation for $\in_f$.

$$\in_f = 1 - e^{-k_f \cdot p_{CO_2+H_2O} \cdot L_o} \tag{A.4}$$

In Eq. (A.4), the effective absorption coefficient k_f by CO_2 and H_2O gases is given by

$$k_f = \left(\frac{0.78 + 1.6 \cdot y_{H_2O}}{\sqrt{p_{CO_2+H_2O} \cdot L_o}} - 0.1\right) \cdot \left(1 - 0.37 \cdot \frac{T_f}{1000}\right) \tag{A.5}$$

where $y_{H_2}O$ is the volumetric fraction of water vapor in the mixture of temperature T_f [K] and p_{CO_2}+H_2O is the absolute partial pressure [kg$_f$/cm^2, 1 kg$_f$/cm^2 = 98066.5 Pa] of CO_2 and H_2O gases in the mixture. Accordingly to [13], the effective thickness L_o [m] of the gas radiating layer filling the flue is the flue channel width. Note that the definition of h_R by Eq. (A.2) is based on the same temperature difference as the convection heat transfer coefficient h_C. Hence, the heat transfer coefficient h that involves combined convection and radiation modes of heat transfer can be introduced into the analysis of high temperature regenerators, so that

$$h = h_C + h_R \tag{A.6}$$

Eq. (A.6) can be supplemented with an additional term that involves the transverse heat conduction in the matrix material. Then accordingly to [13], the bulk thermal resistance at the gas–matrix interface is given by

$$\frac{1}{\bar{h}} = \frac{1}{h_C + h_R} + \frac{\delta}{3 \cdot \lambda_r} \cdot \varphi^* \tag{A.7}$$

Note, one takes $h_R = 0$ of Eq. (A.7) for air flowing in the regenerator.

A.4. Pressure drop analysis

The pressure drop analysis is based on the conventional modeling [9] for core frictional contribution (which is major) as follows after neglecting the entrance and exit pressure losses due to long flue and the change in momentum rate due to negligible density difference between inlet and outlet.

$$\Delta p = \frac{G^2}{2}\left(\lambda \frac{L}{D_h} \frac{1}{\bar{\rho}}\right) \tag{A.8}$$

The Darcy–Weisbach λ friction factor of Eq. (A.8) is determined by the equation:

$$\lambda = C_f \cdot \mathrm{Re}^m \tag{A.9}$$

where $C_\lambda = 64$ and $m = -1$ for laminar flow in the flue, and $C_\lambda = 0.3164$ and $m = -0.25$ when the flow is turbulent. For the actual regenerator an approximation $\bar{\rho} \approx (\rho_i + \rho_o)/2$ holds.

A.5. Thermophysical properties of the gases applied for the case study

The computational analysis presented in the paper uses data describing enthalpy given in [20] for the ideal gases and the mixture enthalpy (expressed per unit mass) is calculated by summation of individual component enthalpies weighted by corresponding mass fractions of the components in the mixture. The mixture mass density is determined using equation of state as for mixture of ideal gases. The other thermophysical properties like viscosity are calculated based on formulae presented in [21] where a mixture property is dependent on

corresponding property, mass fractions and critical properties of the mixture components and temperature of the mixture.

Appendix B. Overall description of the Newton–Raphson algorithm and accuracy of analysis of the model equation system for the case study

The modeling of actual and internal regenerator thus results into solving 78 linear and nonlinear coupled equations for 78 unknowns. We have used an iterative Newton–Raphson [11] method to solve these equations by expanding the nonlinear equations in a first order Taylor series with an assumed starting guess. The resultant linearized equations system is then solved and the iterative process continuously progresses until desired accuracy is achieved.

B.1. The Newton–Raphson algorithm

For the problem to be solved equation system shown in Tables 2 and 4 can be symbolically written as:

$$\left.\begin{array}{l} f_1(X_1,\ldots,X_{78})=0 \\ f_2(X_1,\ldots,X_{78})=0 \\ \vdots \\ f_{78}(X_1,\ldots,X_{78})=0 \end{array}\right\}=0 \tag{B.1}$$

where each function $f_i(X_1,\ldots,X_{40})$, for $i=1,\ldots,N=78$, corresponds to particular equations of Tables 2 and 4 and contains variables $X_1,\ldots,X_{78}$ whose values are just the unknowns as described in Tables 1 and 3. For an iterative Newton–Raphson method [11], equation system (B.1) is expanded in a first order Taylor series with $\boldsymbol{X}_0$ as a starting guess for the solution. Denoting by $\boldsymbol{X}$ the vector of X_j values, where $j=1,\ldots,N$, the expansion of the ith function of system (B.1) in Taylor series in the neighborhood $\boldsymbol{X}-\boldsymbol{X}_0$ of the starting guess $\boldsymbol{X}_0$ gives:

$$f_i(\boldsymbol{X})=f_i(\boldsymbol{X}_0)+\sum_{j=1}^{N}\frac{\partial f_i(\boldsymbol{X}_0)}{\partial X_j}\delta X_{j,0}+R(\delta\boldsymbol{X}_0^2)+\cdots \tag{B.2}$$

where $\delta\boldsymbol{X}_0=[\boldsymbol{X}-\boldsymbol{X}_0]$ is the vector of corrections. Neglecting in (B.2) terms of order $\delta\boldsymbol{X}_0^2$ and higher, and taking into account that accordingly to Eq. (B.1), each function $f_i(\boldsymbol{X})$ should be zeroed, one obtains a set of linear equations with respect to corrections $\delta\boldsymbol{X}_0$. Solution of this system yields the vector of corrections $\delta\boldsymbol{X}_0$ for the starting guess $\boldsymbol{X}_0$ that move all functions $f_i(X_1,\ldots,X_{78})$, for $i=1,\ldots,N=78$, of system (B.1) closer to zero simultaneously after the first iteration. In matrix notation the approach can be written as:

$$\boldsymbol{A}_k\cdot\delta\boldsymbol{X}_k=-\boldsymbol{f}(\boldsymbol{X}_k) \tag{B.3}$$

where the subscript k is introduced to denote the kth iteration and in the notation applied $\delta\boldsymbol{X}_k$ is the entire vector of the corrections for values $\boldsymbol{X}_k$ on stage of the kth iteration. The matrix A_k consists of the first derivatives of each equation of (B.1) system with respect to variables $\boldsymbol{X}$. For the kth current iteration, it can be written as

$$\boldsymbol{A}_k=\left[\frac{\partial f_i(\boldsymbol{X})}{\partial X_j}\right]_{\boldsymbol{X}=\boldsymbol{X}_k} \tag{B.4}$$

However, because of complexity of the expressions involved it is not feasible to compute the first derivatives of (B.4) analytically. Here, partial derivatives (B.4) have been approximated by the forward difference representation.

Having in mind that $\delta\boldsymbol{X}_k=[\boldsymbol{X}-\boldsymbol{X}_k]$, one yields $\boldsymbol{X}_{k+1}=[\boldsymbol{X}_k+\delta\boldsymbol{X}_k]$ as a starting point for the next iteration. Consequently, by determining coefficients according to Eq. (B.4), the expansion about $\boldsymbol{X}_{k+1}$ is performed now, and the equation system (B.3) with new values of $\boldsymbol{A}$ and $\boldsymbol{f}(\boldsymbol{X})$ is solved again. Iterations are continued until a solution satisfies an established convergence accuracy so that the iterative process stops on the kth stage if:

- the maximum absolute value of the corrections $\delta X_{j,k}$, $j=1,\ldots,N$, is less than or equal some assumed tolerance tol_X, hence

$$\max\left\lfloor \mathrm{abs}(\delta X_{j,k})\right\rfloor \leqslant \mathrm{tol}_X,\quad \text{where } j=1,\ldots,78 \tag{B.5}$$

- or the sum of absolute values (residues) of functions $f_i(X_{1,k},\ldots,X_{78,k})$, $i=1,\ldots,N$, of equations system (B.1) is less than or equal some assumed tolerance tol_f, thus

$$\mathrm{res}_{f,k}=\sum_{i=1}^{N}\mathrm{abs}(f_i(X_{1,k},\ldots,X_{78,k}))\mathrm{tol}_\mathrm{f},\quad \text{where } i=1,\ldots,78 \tag{B.6}$$

The results presented in the paper were obtained by checking the convergence with respect to both Eqs. (B.5) and (B.6). Note that the Gauss–Jordan method [11] was employed to solve the equation set (B.3).

B.2. The accuracy of analysis of the model equation system

Because of nonlinearity of the model equations system, two aspects (mathematical convergence, and physical correctness and accuracy) of the results obtained have been verified. Results of a series of numerical experiments confirmed that for the considered case of the model equations system, either under convection

transfer mode or convection and radiation transfer modes combined, the iterative process based on the Newton–Raphson algorithm convergences with respect to:

- absolute values of the right-side residues in the system of model equations (B.1),
- corrections that move all the unknowns in the model equations closer to the solution after each iteration step.

We assumed that inaccuracy of the solution of the equation system (B.1) should be not poorer than 5×10^{-6} as measured by the maximum absolute value of the corrections normalized with respect to the corresponding related variables. The normalized inaccuracy for the kth stage of iteration can be written as

$$\overline{\mathrm{tol}}_{X,k} = \mathrm{MAX}\left[\mathrm{abs}\left(\delta X_{j,k}/X_{j,k}\right)\right] \leqslant 5\cdot10^{-6}, \quad \text{where } j = 1,\ldots,N \tag{B.7}$$

Subsequently, series of numerical experiments were carried out in order

- to investigate how the number of performed iterations affects convergence of the iterative process measured by $\mathrm{res}_{f,k}$ defined by Eq. (B.6), and
- to find out allowed value of $\mathrm{res}_{f,k}$ at which the inaccuracy defined by (B.7) cannot be poorer.

In Figs. B.1 and B.2, the results of numerical experiments are presented where the convergence is illustrated by two limiting curves indicated in either figure. The convergence curves for all the other cases considered in the paper are bounded in between two limiting curves. For the convection mode, one can see

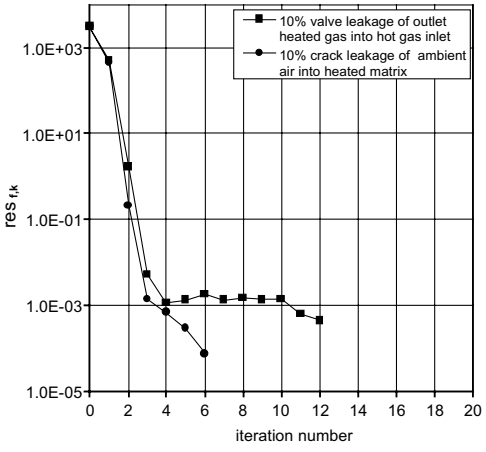

Fig. B.1. Convergence of the iterative process determined by Eq. (B.6) under convection transfer mode.

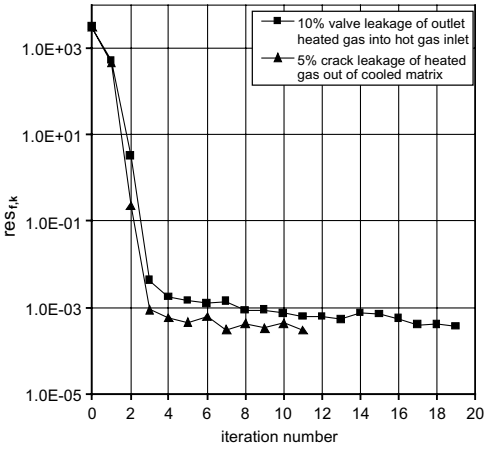

Fig. B.2. Convergence of the iterative process determined by Eq. (B.6) under convection and radiation transfer modes combined.

in Fig. B.1 that the iterative process converges fast and value of $\mathrm{res}_{f,k}$ of Eq. (B.6) becomes lower than 0.001 after four iterations for the case of 10% pressure leakage in the matrix through the crack at left matrix, and after eleven iterations when 10% pressure leakage occurs at hot end valve. It is shown in Fig. B.2 that under the convection and radiation modes combined, the iterative process converges a bit faster when compared to the former case, and the value of $\mathrm{res}_{f,k}$ becomes lower than 0.001 after three iterations for the case of 5% pressure leakage out across the crack at right matrix, and after eight iterations when 10% pressure leakage occurs at hot end valve. Once $\mathrm{res}_{f,k} < 0.001$ for all the cases considered the corresponding maximum inaccuracy was $\overline{\mathrm{tol}}_{X,k} = 3.3\times10^{-6}$ satisfying the criterion expressed by Eq. (B.7). Therefore, we assumed the iterative process has converged to root on the kth stage of iteration if $\mathrm{res}_{f,k} < \mathrm{tol_f} = 0.001$ for all the cases computed. Moreover, as a final check of the problem formulation and physical correctness of the solutions obtained, the regenerator energy transfer imbalance determined with respect to complete operation cycle as composed of the present and former periods has been verified based on the definition

$$\Delta q = \frac{Q_\mathrm{c} - Q_\mathrm{h}}{Q_\mathrm{u}}\cdot 100 \tag{B.8}$$

where Q_c is the amount of heat absorbed from the matrix by the heated gas per complete cycle and Q_h is the amount of heat absorbed by the matrix from the cooled gas per complete cycle. Note that the imbalance expressed by Eq. (B.8) is normalized with respect to useful amount of heat transferred per period. We found based on results of numerical experiments that the maximum value of imbalance expressed by Eq. (B.8) for all the

Table B.1
The starting guess for combined case of pressure leakages across the cracks and valves

Variable		Starting guess for present period	Variable		Starting guess for former period
No.	Symbol		No.	Symbol	
1	$\dot{m}_{a,cr}$	0.1 kg/s	38	$\tilde{\dot{m}}_{c,cr}$	0.11 kg/s
2	$\dot{m}_{c,cr}$	0.1 kg/s	39	$\tilde{\dot{m}}_{a,cr}$	0.11 kg/s
3	$\dot{m}_{c,co}$	0.5 kg/s	40	$\tilde{\dot{m}}_{c,co}$	0.51 kg/s
4	$\dot{m}_{h,co}$	0.5 kg/s	41	$\tilde{\dot{m}}_{h,co}$	0.51 kg/s
5	p_h	−600 Pa	42	$\tilde{p}_c$	550.0 Pa
6	p_c	500 Pa	43	$\tilde{p}_h$	−550.0 Pa
7	$\dot{m}_{h,\upsilon}$	0.5 kg/s	44	$\tilde{\dot{m}}_{h,\upsilon}$	0.51 kg/s
8	$\dot{m}_{c,\upsilon}$	0.5 kg/s	45	$\tilde{\dot{m}}_{c,\upsilon}$	0.51 kg/s
9	$\dot{m}_c$	70 kg/s	46	$\tilde{\dot{m}}_c$	70.1 kg/s
10	$\dot{m}'_c$	69.5 kg/s	47	$\tilde{\dot{m}}'_c$	69.6 kg/s
11	$\dot{m}_{h,CO_2}$	14.8 kg/s	48	$\tilde{\dot{m}}_{h,CO_2}$	14.6 kg/s
12	$\dot{m}_{h,H_2O}$	3.7 kg/s	49	$\tilde{\dot{m}}_{h,H_2O}$	3.5 kg/s
13	$\dot{m}_{h,N_2}$	51.9 kg/s	50	$\tilde{\dot{m}}_{h,N_2}$	51.7 kg/s
14	$\dot{m}_{h,O_2}$	1.9 kg/s	51	$\tilde{\dot{m}}_{h,O_2}$	1.7 kg/s
15	$\dot{m}'_{h,CO_2}$	14.9 kg/s	52	$\tilde{\dot{m}}'_{h,CO_2}$	14.65 kg/s
16	$\dot{m}'_{h,H_2O}$	3.8 kg/s	53	$\tilde{\dot{m}}'_{h,H_2O}$	3.55 kg/s
17	$\dot{m}'_{h,N_2}$	52.0 kg/s	54	$\tilde{\dot{m}}'_{h,N_2}$	51.75 kg/s
18	$\dot{m}'_{h,O_2}$	2.0 kg/s	55	$\tilde{\dot{m}}'_{h,O_2}$	1.75 kg/s
19	$T'_{c,o}$	900.0 °C	56	$\widetilde{T}'_{c,o}$	900.0 °C
20	$T'_{h,o}$	500.0 °C	57	$\widetilde{T}'_{h,o}$	500.0 °C
21	T_c	700.0 °C	58	$\widetilde{T}_c$	700.0 °C
22	T'_c	700.0 °C	59	$\widetilde{T}'_c$	700.0 °C
23	$T'_{h,i}$	1300.0 °C	60	$\widetilde{T}'_{h,i}$	1300.0 °C
24	T_h	800.0 °C	61	$\widetilde{T}_h$	800.0 °C
25	T'_h	799.0 °C	62	$\widetilde{T}'_h$	799.0 °C
26	$\dot{m}_{h,o,CO_2}$	15.0 kg/s	63	$\tilde{\dot{m}}_{h,o,CO_2}$	14.95 kg/s
27	$\dot{m}_{h,o,H_2O}$	3.9 kg/s	64	$\tilde{\dot{m}}_{h,o,H_2O}$	3.95 kg/s
28	$\dot{m}_{h,o,N_2}$	52.1 kg/s	65	$\tilde{\dot{m}}_{h,o,N_2}$	52.0 kg/s
29	$\dot{m}_{h,o,O_2}$	2.1 kg/s	66	$\tilde{\dot{m}}_{h,o,O_2}$	2.05 kg/s
30	$\dot{m}_{c,o,CO_2}$	0.1 kg/s	67	$\tilde{\dot{m}}_{c,o,CO_2}$	0.1 kg/s
31	$\dot{m}_{c,o,H_2O}$	6.0 kg/s	68	$\tilde{\dot{m}}_{c,o,H_2O}$	6.5 kg/s
32	$\dot{m}_{c,o,N_2}$	60.0 kg/s	69	$\tilde{\dot{m}}_{c,o,N_2}$	61.0 kg/s
33	$\dot{m}_{c,o,O_2}$	10.0 kg/s	70	$\tilde{\dot{m}}_{c,o,O_2}$	9.0 kg/s
34	$T_{c,o}$	900.0 °C	71	$\widetilde{T}_{c,o}$	900.0 °C
35	$p_{c,o}$	200.0 Pa	72	$\tilde{p}_{c,o}$	200.0 Pa
36	$T_{h,o}$	500.0 °C	73	$\widetilde{T}_{h,o}$	400.0 °C
37	$p_{h,o}$	−700.0 Pa	74	$\tilde{p}_{h,o}$	−700.0 Pa
Effectiveness (referred to total cycle) of particular parts of the internal regenerator					
75	$\varepsilon_i^{(1)}$	0.8	77	$\varepsilon_i^{(3)}$	0.8
76	$\varepsilon_i^{(2)}$	0.8	78	$\varepsilon_i^{(4)}$	0.8

cases considered in the paper falls below the sufficiently low limit, i.e. $\Delta q < 2 \times 10^{-4}\%$ accompanied as well by inaccuracy $\overline{\mathrm{tol}}_X <= 5.0 \times 10^{-6}$. This indicates that equation system (B.1) has been solved at a reasonable accurate approximation and the solutions obtained turned out to be unique and correct from the physical sense point of view. Note also that number of iterations necessary to solve equation system (B.1) at the above assumed accuracy was on average not more than 20, but for some cases this number was lower to be about 10.

To assume a starting guess X_0, some trials were performed aimed to indicate where that putative root does exist nearby. Based on experience gained and knowledge in physical limitations of particular variables, the guess X_0 was established as shown as an example in Table B.1 for the most general case of combined pressure leakages across the cracks and valves.

Appendix C. Tabulated results, Tables C.1–C.5, for the leakage effects on the regenerator performance.

Table C.1
Effect of valve pressure leakages on performance of the regenerator at pressure leakage factors of 5% and 10%

Parameters	Convection transfer mode					Convection and radiation transfer modes combined				
	0% pressure leakage	5% leakage factor		10% leakage factor		0% pressure leakage	5% leakage factor		10% leakage factor	
		Leaking cold end valve	Leaking hot end valve	Leaking cold end valve	Leaking hot end valve		Leaking cold end valve	Leaking hot end valve	Leaking cold end valve	Leaking hot end valve
Internal regenerator										
$T'_{h,i}$ [°C]	1300	1300	1290	1300	1282	1300	1300	1291	1300	1283
$T'_{h,o}$ [°C]	417	439	439	463	460	405	428	430	453	453
$T'_{c,o}$ [°C]	1068	1094	1079	1121	1089	1079	1105	1087	1131	1096
C_h [kW/K]	87.10	87.29	91.35	87.49	95.62	86.88	87.09	91.16	87.32	95.45
C_c [kW/K]	78.62	74.85	78.69	71.06	78.75	78.78	74.99	78.83	71.18	78.88
C^*	0.903	0.858	0.861	0.812	0.824	0.907	0.861	0.865	0.815	0.826
C_r^*	4.997	5.249	4.993	5.529	4.990	4.987	5.239	4.984	5.520	4.981
NTU_o	3.884	4.046	3.956	4.222	4.026	4.091	4.261	4.111	4.445	4.153
$\varepsilon_{i,b}$	0.8207	0.8412	0.8358	0.8616	0.8494	0.8283	0.8489	0.8414	0.8692	0.8539
Actual regenerator										
Δp_h [Pa]	515	526	570	538	629	510	522	567	535	626
Δp_c [Pa]	372	352	379	331	386	373	354	381	334	388
$T_{h,o}$ [°C]	417	423	438	431	459	405	413	430	422	453
$T_{c,o}$ [°C]	1068	1094	1079	1121	1089	1079	1105	1087	1132	1096
Q [GJ/period]	415	406	420	395	425	420	411	424	400	428
Q_u [GJ/period]	415	406	399	396	382	420	411	403	400	385
ε_b	0.7941	0.7763	0.7632	0.7563	0.7309	0.8037	0.7855	0.7704	0.7650	0.7367
$\dot{m}_{c,o}$ [kg/s]	69.99	66.49	66.49	62.99	62.99	69.99	66.49	66.49	62.99	62.99
$\dot{m}_{h,o}$ [kg/s]	70.01	73.51	73.51	77.01	77.01	70.01	73.51	73.51	77.01	77.01
$\dot{m}_{c,co}$ [kg/s]	0.0413	0.0403	0.0406	0.0393	0.0400	0.0411	0.0401	0.0405	0.0391	0.0399
$\dot{m}_{h,co}$ [kg/s]	0.0315	0.0310	0.0310	0.0304	0.0305	0.0317	0.0311	0.0311	0.0305	0.0306
$\dot{m}_{c,v}$ [kg/s]	0	3.5	0	7.0	0	0	3.5	0	7.0	0
$\dot{m}_{h,v}$ [kg/s]	0	0	3.5	0	7.0	0	0	3.5	0	7.0
$\dot{m}_{a,cr}$ [kg/s]	0	0	0	0	0	0	0	0	0	0
$\dot{m}_{c,cr}$ [kg/s]	0	0	0	0	0	0	0	0	0	0

Table C.2
Effect of crack pressure leakages on performance of the regenerator at leakage factor of 5% under convection transfer mode

Parameters	Pressure leakage factor under present period									
	0% pressure leakage	Leaking in heated regenerator at leakage factor of 5%				Leaking out cooled regenerator at leakage factor of 5%				
		Heated regenerator			Cooled regenerator	Cooled regenerator				Heated regenerator
Internal regenerator										
$T'_{h,i}$ [°C]	1300		1300		1300[a]		1300[a]			1300
$T'_{h,o}$ [°C]	417		419		417[a]		420[a]			417
$T'_{c,o}$ [°C]	1068		1056[a]		1068		1049			1068[a]
		Part 1 (upper)		Part 2 (lower)		Part 4 (upper)		Part 3 (lower)		
C_h [kW/K]	87.10	91.46		89.32	87.10[a]	91.43[a]		91.86[a]		87.10
C_c [kW/K]	78.62	81.15[a]		76.71[a]	78.62	79.25		76.55		78.62[a]
C^*	0.903	0.887		0.859	0.903	0.867		0.833		0.903
C_r^*	4.997	1.210		3.842	4.998	1.239		3.850		4.998
NTU_o	3.884	1.198		2.652	3.884	1.211		2.645		3.884
$\varepsilon_{i,b}$	0.8207	0.5135		0.7556	0.8207	0.5200		0.7613		0.8207
Actual regenerator			Present period	Former period			Present period	Former period		
Δp_h [Pa]	515		542	515			515	561		
Δp_c [Pa]	372		372	361			353	372		
$T_{h,o}$ [°C]	417		419	417			417	420		
$T_{c,o}$ [°C]	1068		1068	1056			1049	1068		
Q [GJ/period]	415		415	406			400	415		
Q_u [GJ/period]	415		415	398			387	415		
ε_b	0.7941		0.7941	0.7609			0.7388	0.7941		
$\dot{m}_{c,o}$ [kg/s]	69.99		69.99	67.95			66.49	69.99		
$\dot{m}_{h,o}$ [kg/s]	70.01		73.51	70.01			70.01	75.94		
$\dot{m}_{c,co}$ [kg/s]	0.0413		0.0422	0.0413			0.0413	0.0428		
$\dot{m}_{h,co}$ [kg/s]	0.0315		0.0315	0.0321			0.0325	0.0315		
$\dot{m}_{c,\upsilon}$ [kg/s]	0		0	0			0	0		
$\dot{m}_{h,\upsilon}$ [kg/s]	0		0	0			0	0		
$\dot{m}_{a,cr}$ [kg/s]	0		3.5	0			0	5.93		
$\dot{m}_{c,cr}$ [kg/s]	0		0	2.04			3.5	0		

[a] Data referring to former period.

Table C.3
Effect of crack pressure leakages on performance of the regenerator at leakage factor of 10% under convection transfer mode

Parameters	Pressure leakage factor under present period								
	0% pressure leakage	Leaking in heated regenerator at leakage factor of 5%				Leaking out cooled regenerator at leakage factor of 5%			
		Heated regenerator			Cooled regenerator	Cooled regenerator			Heated regenerator
Internal regenerator									
$T'_{h,i}$ [°C]	1300		1300		1300[a]		1300[a]		1300
$T'_{h,o}$ [°C]	417		420		417[a]		421[a]		417
$T'_{c,o}$ [°C]	1068		1047[a]		1068		1038		1068[a]
		Part 1 (upper)		Part 2 (lower)		Part 4 (upper)		Part 3 (lower)	
C_h [kW/K]	87.10	91.42		92.98	87.10[a]	91.37[a]		97.68[a]	87.10
C_c [kW/K]	78.62	78.40[a]		76.48[a]	78.62	74.79		76.21	78.61[a]
C^*	0.903	0.858		0.823	0.903	0.819		0.780	0.903
C_r^*	4.997	1.253		3.853	4.998	1.313		3.867	4.998
NTU_o	3.884	1.217		2.643	3.884	1.243		2.633	3.884
$\varepsilon_{i,b}$	0.8207	0.5229		0.7637	0.8207	0.5361		0.7731	0.8207
Actual regenerator			Present period	Former period			Present period	Former period	
Δp_h [Pa]	515		570	515			515	607	
Δp_c [Pa]	372		372	350			339	371	
$T_{h,o}$ [°C]	417		420	417			417	421	
$T_{c,o}$ [°C]	1068		1068	1047			1038	1068	
Q [GJ/period]	415		415	398			388	415	
Q_u [GJ/period]	415		415	382			361	415	
ε_b	0.7941		0.7941	0.7293			0.6907	0.7941	
$\dot{m}_{c,o}$ [kg/s]	69.99		69.99	65.83			62.99	69.99	
$\dot{m}_{h,o}$ [kg/s]	70.01		77.01	70.01			70.01	81.52	
$\dot{m}_{c,co}$ [kg/s]	0.0413		0.0431	0.0413			0.0413	0.0441	
$\dot{m}_{h,co}$ [kg/s]	0.0315		0.0315	0.0327			0.0334	0.0315	
$\dot{m}_{c,v}$ [kg/s]	0		0	0			0	0	
$\dot{m}_{h,v}$ [kg/s]	0		0	0			0	0	
$\dot{m}_{a,cr}$ [kg/s]	0		7.0	0			0	11.51	
$\dot{m}_{c,cr}$ [kg/s]	0		0	4.16			7.0	0	

[a] Data referring to former period.

Table C.4
Effect of crack pressure leakages on performance of the regenerator at leakage factor of 5% under convection and radiation transfer modes combined

Parameters	Pressure leakage factor under present period								
	0% pressure leakage	Leaking in heated regenerator at leakage factor of 5%				Leaking out cooled regenerator at leakage factor of 5%			
		Heated regenerator			Cooled regenerator	Cooled regenerator			Heated regenerator
Internal regenerator									
$T'_{h,i}$ [°C]	1300		1300		1300[a]		1300[a]		1300
$T'_{h,o}$ [°C]	405		410		405[a]		412[a]		405
$T'_{c,o}$ [°C]	1079		1065[a]		1079		1058		1079[a]
		Part 1 (upper)		Part 2 (lower)		Part 4 (upper)		Part 3 (lower)	
C_h [kW/K]	86.88	91.43		89.18	86.88[a]	91.39[a]		91.70[a]	86.88
C_c [kW/K]	78.78	81.20[a]		76.71[a]	78.78	79.29		76.54	78.78[a]
C^*	0.907	0.888		0.860	0.907	0.868		0.835	0.907
C_r^*	4.987	1.210		3.841	4.987	1.239		3.850	4.987
NTU_o	4.091	1.290		2.741	4.091	1.301		2.717	4.091
$\varepsilon_{i,b}$	0.8283	0.5311		0.7623	0.8283	0.5373		0.7668	0.8283
Actual regenerator			Present period	Former period			Present period	Former period	
Δp_h [Pa]	510		537	510			510	556	
Δp_c [Pa]	373		373	361			353	373	
$T_{h,o}$ [°C]	405		410	405			405	412	
$T_{c,o}$ [°C]	1079		1079	1065			1058	1079	
Q [GJ/period]	420		420	410			404	420	
Q_u [GJ/period]	420		421	402			390	420	
ε_b	0.8037		0.8038	0.7686			0.7459	0.8037	
$\dot{m}_{c,o}$ [kg/s]	69.99		69.99	67.95			66.49	69.99	
$\dot{m}_{h,o}$ [kg/s]	70.01		73.51	70.01			70.01	75.93	
$\dot{m}_{c,co}$ [kg/s]	0.0411		0.0422	0.0411			0.0411	0.0428	
$\dot{m}_{h,co}$ [kg/s]	0.0317		0.0317	0.0323			0.0328	0.0317	
$\dot{m}_{c,\upsilon}$ [kg/s]	0		0	0			0	0	
$\dot{m}_{h,\upsilon}$ [kg/s]	0		0	0			0	0	
$\dot{m}_{a,cr}$ [kg/s]	0		3.5	0			0	5.92	
$\dot{m}_{c,cr}$ [kg/s]	0		0	2.04			3.5	0	

[a] Data referring to former period.

Table C.5
Effect of crack pressure leakages on performance of the regenerator at leakage factor of 10% under convection and radiation transfer modes combined

Parameters	Pressure leakage factor under present period							
	0% pressure leakage	Leaking in heated regenerator at leakage factor of 5%			Leaking out cooled regenerator at leakage factor of 5%			
		Heated regenerator		Cooled regenerator	Cooled regenerator		Heated regenerator	
Internal regenerator								
$T'_{h,i}$ [°C]	1300	1300		1300[a]	1300[a]		1300	
$T'_{h,o}$ [°C]	405	413		405[a]	414[a]		405	
$T'_{c,o}$ [°C]	1079	1055[a]		1079	1046		1079[a]	
		Part 1 (upper)	Part 2 (lower)		Part 4 (upper)	Part 3 (lower)		
C_h [kW/K]	86.88	91.37	92.83	86.88[a]	91.32[a]	97.50[a]	86.88	
C_c [kW/K]	78.78	78.43[a]	76.46[a]	78.78	74.81	76.18	78.78[a]	
C^*	0.907	0.858	0.824	0.907	0.819	0.781	0.907	
C_r^*	4.987	1.252	3.854	4.987	1.313	3.868	4.987	
NTU_o	4.091	1.308	2.710	4.091	1.332	2.680	4.091	
$\varepsilon_{i,b}$	0.8283	0.5405	0.7689	0.8283	0.5532	0.7768	0.8283	
Actual regenerator			Present period	Former period		Present period	Former period	
Δp_h [Pa]	510		564	510		510	601	
Δp_c [Pa]	373		373	350		338	373	
$T_{h,o}$ [°C]	405		413	405		405	414	
$T_{c,o}$ [°C]	1079		1079	1055		1046	1079	
Q [GJ/period]	420		420	402		391	420	
Q_u [GJ/period]	420		421	385		365	420	
ε_b	0.8037		0.8039	0.7362		0.6971	0.8037	
$\dot{m}_{c,o}$ [kg/s]	69.99		69.99	65.83		62.99	69.99	
$\dot{m}_{h,o}$ [kg/s]	70.01		77.01	70.01		70.01	81.49	
$\dot{m}_{c,co}$ [kg/s]	0.0411		0.0431	0.0411		0.0411	0.0442	
$\dot{m}_{h,co}$ [kg/s]	0.0317		0.0317	0.0329		0.0336	0.0315	
$\dot{m}_{c,\upsilon}$ [kg/s]	0		0	0		0	0	
$\dot{m}_{h,\upsilon}$ [kg/s]	0		0	0		0	0	
$\dot{m}_{a,cr}$ [kg/s]	0		7.0	0		0	11.48	
$\dot{m}_{c,cr}$ [kg/s]	0		0	4.16		7.0	0	

[a] Data referring to former period.

Appendix D. Practical correlation for calculations of the leakage effect

In this Appendix, we propose a simple correlation that can be used in engineering practice to evaluate the drop in actual regenerator effectiveness due to leakages. It has been shown in the paper that the radiation transfer affects negligibly the leakage effect as well as leakage of ambient air into heated regenerator can be disregarded. Then, data used to develop the correlation are those obtained for the convection transfer mode and involve the most important effects as follows:

- crack leakage (heated air) out of the cooled regenerator,
- cold end valve leakage of cold (heated) gas at its inlet to the cooled matrix into hot gas at its outlet from the heated matrix, and
- hot end valve leakage of cold (heated) gas at its outlet from the cooled matrix into hot gas at the inlet to the heated matrix.

All the data taken into considerations are shown in Table D.1.

Table D.1
Data points on drop in actual regenerator effectiveness due to various leakages

Point number	Amount of leakages by leakage factors, %		Drop in actual regenerator effectiveness, %
	Crack leakage	Cold/hot end valve leakage	
1	0	0/0	0
2	2.91	0/0	3.32
3	5.0	0/0	5.53
4	5.94	0/0	6.48
5	10.0	0/0	10.34
6	0	5.0/0	1.78
7	0	5.06/0	1.80
8	0	10.0/0	3.78
9	0	0/5.0	3.09
10	0	0/10.0	6.32
11	5.0	5.0/0	7.47
12	5.0	5.0/5.0	10.83
13	2.86	4.97/5.02	8.49
14	5.76	10.35/9.98	17.90
15	10.03	10.25/10.08	22.33

It is seen from Figs. 6 and 7 that the drop in ε_b due to leakages are almost linear, so we selected the following form of the correlation:

$$\Delta\varepsilon_b = a_1 \cdot \ell_{c,cr} + a_2 \cdot \ell_{c,\upsilon} + a_3 \cdot \ell_{h,\upsilon} \tag{D.1}$$

In Eq. (D.1), a_1, a_2 and a_3 are adjustable parameters to be determined based on data of Table D.1, and various ℓ's are the leakage factors (%) defined as:

$$\ell_{c,cr} = \frac{\dot{m}_{c,cr}}{l_{tot}} \cdot 100 \quad \ell_{c,\upsilon} = \frac{\dot{m}_{c,\upsilon}}{l_{tot}} \cdot 100$$
$$\ell_{h,\upsilon} = \frac{\dot{m}_{h,\upsilon}}{\ell_{tot}} \cdot 100 \tag{D.2}$$

where the total pressure leakage of the cold heated gas l_{tot} into the hot cooled gas is given by

$$l_{tot} = \dot{m}_{c,cr} + \dot{m}_{c,\upsilon} + \dot{m}_{h,\upsilon} \tag{D.3}$$

By using the least squares method to fit the data points given in Table D.1 to Eq. (D.1) one arrives at the following correlation describing drop in actual regenerator effectiveness due to various leakages

$$\Delta\varepsilon_b = 1.0890 \cdot \ell_{c,cr} + 0.4151 \cdot \ell_{c,\upsilon} + 0.6828 \cdot \ell_{h,\upsilon} \tag{D.4}$$

Eq. (D.4) correlates the drop with ±0.3% accuracy measured by the standard deviation of values from data given in Table D.1. Note also that the correlation coefficient for the fitting Eq. (D.4) is 0.99, which indicates that the values of the drop and leakages factors are almost perfectly correlated by Eq. (D.4). In Fig. D.1, trends in the drop vs. leakage factors are shown. The linear increase in $\Delta\varepsilon_b$ with leakages is clearly demonstrated.

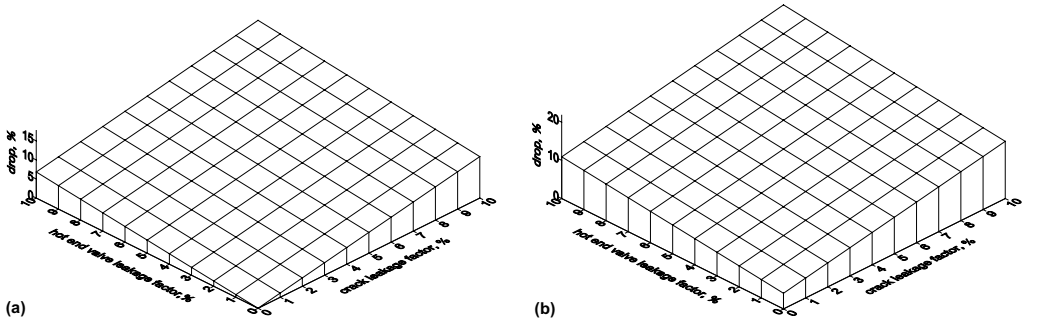

Fig. D.1. Drop in actual regenerator effectiveness due to various leakages determined based on correlation of Eq. (D.4): (a) the case of 0%, and (b) the case of 10% cold end valve leakage factor.

References

[1] D.B. Harper, W.M. Rohsenow, Effect of rotary regenerator performance on gas-turbine-plant performance, Trans. ASME 75 (1953) 759–765.

[2] P.J. Banks, W.M.J. Ellul, Predicted effects of by-pass flows on regenerator performance, Mechanical & Chemical Engineering Transactions MC, vol. 9 (1–2), The Institution of Engineers, Australia, 1973, pp. 10–14.

[3] P.J. Banks, The representation of regenerator fluid carry-over by bypass flows, ASME J. Heat Transfer 106 (1984) 216–220.

[4] T. Skiepko, Indirect estimation of leakage distribution in steam boiler rotary regenerators, Heat Transfer Eng. 18 (1) (1997) 56–81.

[5] R.K. Shah, T. Skiepko, Influence of leakage distribution on the thermal performance of a rotary regenerator, in: Proceedings of the 4th World Conference on Experimental Heat Transfer, Fluid Mechanics and Thermodynamics, vol. 1, Edizioni ETS, Italy, 1997, pp. 365–377.

[6] T. Busby, Can regenerator packing research lead to more efficient furnaces? Glass Ind. (12) (1991) 29–32.

[7] J. Wrona, E. Witek, Regenerator—its significance for proper working of glass melting furnace and operation problems, Manage. Fuels Energy Sources (in Polish: Gospodarka Paliwami i Energi(ca)) (12) (1994) 20–23.

[8] R.K. Shah, T. Skiepko, Modeling of leakages in fixed-matrix regenerators, in: Proceedings of the 11th International Heat Transfer Conference, vol. 6, 1998, pp. 233–238.

[9] W.M. Kays, A.L. London, Compact Heat Exchangers, third ed., McGraw-Hill, New York, 1984, p. 31.

[10] R.K. Shah, D.P. Sekulić, Fundamentals of Heat Exchanger Design, John Wiley & Sons, New York, 2003, Chapter 5.

[11] W.H. Press, B.P. Flannery, S.A. Teukolsky, W.T. Vetterling, Numerical Recipes, The Art of Scientific Computing, first ed., Cambridge University Press, Cambridge, 1986, p. 269.

[12] B. Kulakowski, Explicit design of balanced regenerators, in: G.F. Hewitt (Ed.), Heat Exchanger Design Handbook 1998, Begell House Inc., New York, 1998, Sec. 3.15.11.

[13] F.W. Schmidt, A.J. Willmott, Thermal Energy Storage and Regeneration, Hemisphere, Washington, 1981, p. 164.

[14] P. Razelos, V. Parkis, The thermal design of blast furnace stove regenerators, Iron Steel Engr. 22 (9) (1968) 81–116.

[15] N.V. Kuznetsov et al. (Eds.), Thermal Analysis of Steam Boilers, Standard Method, Energija, Moskva, 1973, p. 43.

[16] H. Hausen, Wärmeübertragung im Gegenstrom, Gleichstrom und Kreuzstrom, Springer-Verlag, Berlin, 1950, p. 316.

[17] Z.H. Lin, Thermohydraulic design of fossil-fuel-fired boiler components, in: S. Kakaç (Ed.), Boilers, Evaporators and Condensers, John Wiley & Sons, New York, 1991, Chapter 8.

[18] H.C. Hottel, R.B. Egbert, Radiant heat transmission from water vapor, Trans. Amer. Inst. Chem. Eng. 38 (1942) 531–568.

[19] A.M. Gurvič, V.V. Mitor, Radiation of combustion gases, Teploenergetika (12) (1955) 28–31.

[20] Y.A. Çengel, M.A. Boles, Thermodynamics, An Engineering Approach, first ed., McGraw-Hill, New York, 1989, Appendix 1.

[21] R.C. Reid, J.M. Prausnitz, T.K. Sherwood, The Properties of Gases and Liquids, third ed., McGraw-Hill, 1976.